

DETECTION AND IDENTIFICATION OF VIRUSES  
BY CAPILLARY ISOELECTRIC FOCUSING

By

MUKUND B. KOIRALA

B.Sc., Amrit Science College, 1994

M.Sc., Tribhuvan University, 1997

A THESIS

Submitted in partial fulfillment of the requirements for the degree

MASTER OF SCIENCE

Department of Chemistry  
College of Arts and Sciences

KANSAS STATE UNIVERSITY  
Manhattan, Kansas

2014

Approved by:

Major Professor  
Dr Christopher Culbertson

# **Copyright**

MUKUND B KOIRALA

2014

## **Abstract**

Capillary isoelectric focusing (cIEF) is one of several electrophoretic separation techniques for proteins and various other bio - molecules widely used in biochemistry laboratories. A wide range of analytes separable by the different modes of Capillary Electrophoresis (CE) includes from a small organic or an inorganic molecule to the complex bio-molecules such as protein, peptides, cell organelles, and live microorganisms (e.g. bacteria and viruses). Of the various modes of electrophoresis, Isoelectric focusing (IEF) is a good method for the separation of large amphoteric molecules such as peptides and proteins because of the attainment of overall surface charge depending up on its environment pH.

This thesis mainly focuses on application of cIEF for proteins separation and viruses' detection, which is one of the biggest concerns of human and animal health because of viral outbreak causing loss of thousands of lives and property every year. In Chapter one of this thesis, the principles and mechanisms of separation of CE, cIEF, comparative advantages of dynamic coatings over static coating, and advantages of Whole Column Imaging Detection (WCID) over On - olumn Single Point Detection have been discussed . Chapter two includes experimental procedure and calculations for EOF determination. The results of cIEF experiments with standard proteins to develop calibration curve followed by UV absorbance detection of two bacteriophage viruses TR4 and T1 are presented in the Chapter three. Final Chapter four includes the conclusion and discussion on future direction for the project.

The main motivation for this work was to develop a method which is less labor intensive and requires shorter detection time compared to traditional detection methods such

as virus culture in serology (7days), polymerase chain reaction (PCR) and gel electrophoresis (6hrs to 2days) . A commercially available dynamic coating reagent, EoTrol LN® copolymer used our CE experiments found to be more convenient and efficient than commonly used surface modifiers for example silane-based reagents. Preliminary determination of the pIs of these T1 and TR4 by cIEF was  $3.1 \pm 1.0$  and  $6.8 \pm 1.0$  respectively. The pI of viruses can differ by their strains and the phase of virus - growth. The viruses, though closely related, are easily distinguishable by their different pIs.

# Table of Contents

Abstract .....	iii
List of Figures .....	vii
List of Tables .....	ix
Acknowledgements .....	x
Dedication .....	xi
Chapter 1 - Capillary Electrophoresis .....	1
Introduction .....	1
1.1 Principles of CE .....	5
1.1.1 Electrophoresis .....	5
1.1.2 Electroosmosis .....	8
1.1.3 Separation Efficiency .....	12
1.1.4 Resolution in CE .....	13
1.1.5 Advantages of CE .....	14
1.1.6 Modes of sample Injections .....	15
1.1.6.1 Electrokinetic injection .....	15
1.1.6.2 Hydrodynamic sample injection .....	16
1.2 Source of band broadening in cIEF .....	17
1.2.1 Molecular diffusion .....	18
1.2.2 Adsorption on surface .....	19
1.2.3 Effects of voltage and temperature .....	19
1.2.4 Detection-window band broadening .....	20
1.3 Instrumentation .....	24
1.4 Modes of CE .....	25
1.5 Capillary Isoelectric Focusing (cIEF) .....	26
1.5.1 Establishing pH gradient .....	28
1.5.2 Carrier Ampholytes .....	29
1.5.3 Amino acids and proteins .....	30
1.7.1 Resolution of cIEF .....	32

1.6 Detection .....	33
1.8.1 On-column single point detection.....	33
1.8.2 Whole column imaging detection .....	35
1.8.3 Online cIEF- MS detection .....	36
1.7 Mobilization.....	37
1.7.1 Anodic mobilization.....	37
1.7.2 Cathodic mobilization .....	38
1.7.3 Pressure mobilization.....	39
1.7.4 Advantages cIEF .....	40
1.8 Capillary surface coating .....	41
1.8.1 Dynamic Coating .....	42
1.8.2 Covalent coating .....	44
1.9 Viruses .....	45
1.9.1 Structure of viruses .....	47
Chapter 2 - Experimental Procedures .....	50
2.1 Materials and Methods.....	50
2.2 Solution Preparation.....	51
2.3 Capillary cutting, preconditioning .....	52
2.4 Dynamic coating procedure .....	53
2.5 Capillary Electrophoresis: injection mode and run time.....	53
2.6 EOF determination.....	54
2.6.1 Experimental Setup.....	56
2.6.2 Detection .....	57
2.6.3 Isoelectric focusing of proteins .....	58
2.6.4 Mobilization procedure of proteins.....	59
Chapter 3 - Coatings efficiency via EOF determination.....	60
3.1 CE of RhB and Rh6G <sup>+</sup> without and with silane-based reagent coating.....	60
3.2 CE of RhB and Rh6G <sup>+</sup> with EoTrol LN® coating.....	64
3.3 cIEF of proteins and Viruses.....	65
Chapter 4 - Conclusions and future directions.....	71
References.....	73

## List of Figures

Fig 1.1: Forces acting on a particle in fluid flowing under the influence of electric field .....	6
Fig 1.2: Schematic of electrophoretic ( $v_{ep}$ ), electroosmotic flow ( $v_{eo}$ ) and electrokinetic velocity ( $v_{ek}$ ) of positive and negatively charged ion due to effect of applied electric field on ions. ..	7
Fig 1.3: Schematics of an electrical double layer formation on silica surface and a potential variation in double layer. <sup>15,16</sup> .....	10
Fig 1.4: Illustration of electroosmosis due to application of electric field in a capillary. <sup>17</sup> .....	11
Fig 1.5: Illustration of resolution of a peak, peak width at half maxima and base line width .....	13
Fig 1.6: Illustration of electrokinetic Injection of sample into a capillary for CE.....	15
Fig 1.7: Illustration of irradiation $I_0$ of a sample on cylindrical optical path (A) and rectangular path (B) absorbance by a sample. <sup>21</sup> .....	21
Fig 1.8: Illustration of Z - cell (A) and bubble cell (B) for UV/VIS absorption detection sensitivity enhancement. <sup>24</sup> .....	22
Fig 1.9: Jablonski diagram to illustrate absorption and fluorescence phenomena in Laser induced Fluorescence detection method. <sup>28</sup> .....	23
Fig 1.10: Schematics of experimental setup for CE. <sup>24</sup> .....	25
Fig 1.11: Schematic of isoelectric focusing process. The proteins at pH higher than pI migrate towards anode but a protein at the pH lower than its pI move toward cathode until they attain overall zero net charge. ....	27
Fig 1.12: Titration curve of glycine. <sup>21</sup> .....	31
Fig 1.13: Components of photodiode array detector. <sup>24</sup> .....	34
Fig 1.14: An illustration of concept of Whole Column Imaging Detection (WCID) for cIEF separation. <sup>47</sup> .....	36
Fig 1.15 : Schematics of anodic mobilization of focused proteins bands in cIEF.....	38
Fig 1.16: Schematics of cathodic mobilization of separate protein band in cIEF. ....	39
Fig 1.17: Illustration of layers formation in dynamic coating. <sup>64</sup> .....	43
Fig 1.18: Electron micrograph of bacteriophage T1 virus has polygonal head, neck and tail in Fig labeled A, Tobacco Mosaic virus in B is rod shaped and Rabi's virus has tablet shaped in C and Rota virus is sphere shaped like solid sphere with a lots of spikes on its surface <sup>72,73</sup> ..	46

Fig 1.19: Schematics of structure of viruses. <sup>71</sup> .....	48
Fig 2.1: Experimental set up for cIEF.....	57
Fig 3.1: Electropherogram of RhB and Rh6G <sup>+</sup> obtained by CE with preconditioned capillary without any coating. Migration times of Rh6G <sup>+</sup> and RhB 181 ± 1 s with 0.5 % RSD and 298 ± 8 s with 2.3 % RSD respectively. ....	63
Fig 3.2: Electropherogram RhB and Rh6G <sup>+</sup> mixture obtained by CE of with EoTrol LN® polymer coated capillary. The electropherograms of three consecutive runs with migration time 819 ± 20 s with 2.4 % RSD.....	64
Fig 3.3: Electropherogram of four consecutive runs of IEF of Myoglobin (equine) in an EoTrol LN® coated capillary followed by anodic mobilization with 66% NaCl and 33% NaOH mixture by volume. Mobilization time of Myoglobin is 920 ± 31 s with RSD of 3.4%. ....	66
Fig 3.4: Electropherogram of four consecutive runs of cIEF of Lysozyme in an EoTrol LN® coated capillary followed by anodic mobilization with neutral NaCl solution. Mobilization time of Lysozyme is 299 ± 22 s with % RSD of 7.5.....	67
Figure 3.5 Plot of mobilization time in observed experimentally against the reported pI values of standard proteins. ....	68
Fig 3.6: Electropherogram of three runs of TR4 virus detected by anodic mobilization after cIEF. Mobilization time is 798 ± 17s with 2.2% RSD. ....	69
Fig 3.7: Electropherogram of T1 virus detected by anodic mobilization after cIEF. Migration times is 1450 ± 87 s with 4.4 % RSD, a sharper peak at 1850 ± 20 s.....	69



## List of Tables

Table 1: Summary of migration times and mobilities. ....	61
Table 2: Summary of migration times, % RSD, quality of separation (N), and Resolution (Rs) .....	61
Table 3: Summary contains mobilization time of standard proteins, reported pI range, masses and number of amino acids and charge of the proteins in high and low pH. ....	66
Table 4: Calculation of pI of viruses based on their mobilization times during anodic mobilization. ....	68

## Acknowledgements

It has been four years since I left Nepal. On the one hand, I was very excited by the true feeling of self pride and optimism for a better future, but on the other hand, leaving better half and my two little sweet hearts in the capital city several hundred kilometers away from home town without full confidence of safety and security was a great challenge for me. I had a great enthusiasm pursuing my desired goal of achieving higher education from the university of a developed countries like USA but also great challenges to overcome. First of all I would like to thank and appreciate Prof. Ryszard Jankowiak taking me as his graduate student. And also, the constant moral support and help which Mrs. Majka Jankowiak provided us hope and love during the most difficult times in Kansas. I would like to acknowledge and thank Professor Daniel Higgins accepting request to be in adviser's committee and providing an opportunity to work on single molecule research. I also would like thank chemistry department and faculty for the opportunity to pursue my goals, nourish my thirst for science research at Kansas State University.

Most importantly, I would like thank and acknowledge Professor Christopher Culbertson for guidance and advice. I, also value the friendships with the following people; Khem, Naweem, Arun, Adam, Bhanu, Amita, Eve, Amos, Damith, Kathleen, Sami and Mrs Anne Culberstson. My stay at Manhattan would not have been a pleasant if I had not met the following wonderful people, Judd and Nancy Swihart, Steve and Melanie Graver. The last but not the least, I sincerely acknowledge my better half Devi and adorable children Bhavin and Maitri the warm companionship and energy throughout my life.

## **Dedication**

I would like to dedicate this thesis to my parents Hari B. Koirala and Parbati Devi Koirala who have been always a source of inspiration, love, guidance and encouragement from the time I can remember.

# Chapter 1 - Capillary Electrophoresis

## Introduction

Capillary Electrophoresis (CE) has emerged as a powerful separation tool for proteins and bio - molecules. CE separates analytes based on their differential mobilities under the influence of the electric field.<sup>1</sup> The movement of an analyte in CE is determined by the electrophoretic mobility of the analyte and the electroosmotic mobility of the electrolyte. Near the negatively charged capillary surface, electrolytes flow towards the cathode. This flow is called electroosmotic flow (EOF). If the surface is coated with positive ions, the electroosmotic flow (i.e. EOF) reverses its direction. The electrophoretic mobility of an analyte is the motion of an analyte in an electric field and depends upon the physical characteristics of the analyte itself (e.g. charge, size and shape) and with that of the electrolyte properties (e.g. ionic strength, pH, viscosity and additives). Difference in the electrophoretic mobilities of analytes and the control of the electroosmotic flow are a few of the many parameters upon which a successful separation by CE depends.

In the last few decades, CE has been extensively utilized as an analytical and research tool for studying various bio-molecules and microorganisms.<sup>2</sup> The fundamental principle behind all forms of electrophoresis is the same; i.e. the influence of an electric field on charged molecules.<sup>3</sup> Particularly in CE, analytes of interest are injected into a narrow bore capillary, whose internal diameter is about the same dimension as a human hair (50  $\mu\text{m}$ ). The time taken by the analyte to reach the detection point is known as the migration time. The migration time in capillary electrophoresis is dependent upon both the charge, the size of the analyte and the electroosmotic flow (EOF). The EOF originates in the capillary as a result of charge on the surface. Negative charges on the interior surface arise due to the interaction of the running electrolyte with the

silanol (-SiOH) groups present on the silica surface. Ionization of -SiOH groups on the surface does not occur until the surface comes in contact with an aqueous solution.

The magnitude of the negative charge is dependent on the pH of the solution interfacing with the capillary surface. At more acidic pH, the ionization of silanol groups is suppressed which results a decrease in the surface charge. Using the Henderson-Hasselbalch equation,  $pK_a = pH + \log(\text{base/acid})$ , the ionization state on the capillary surface can be predicted. The number of protonated and deprotonated silanol groups would be equal if pH of the buffer in the capillary were equal to the pKa value of the silanol. If the solution pH is lower than the pKa, most of the silanol groups are protonated. Therefore, there will be less charge on the capillary surface. But for most protein separations, the buffer pH used is between 8 and 9. At this pH, the capillary surface silanol groups are mostly deprotonated i.e. negatively charged. The different magnitude of surface charge leads to different EOF velocity and hence different migration time. A molecule with higher electrophoretic mobility migrates past the detector with a shorter migration time. Although migration time is not an intrinsic property of any analyte, the relative migration times of different molecules under a specific set of experimental conditions can be used to identify an unknown species in the solution. The migration time of a particular analyte is an indirect indication of its mass, charge, size and shape.

Each peak corresponds to a different analyte moving past the detection window. The area of a peak can be related to the concentration of the analyte. A sharper and well resolved peak indicates a high efficiency separation. But in many cases various dispersive forces acting on the molecules cause peak broadening. Peak broadening hinders quality of the separation, efficiency, and the resolution of the peaks.

Furthermore, to achieve simultaneous separation of positive, negative and neutral analyte from a mixture by capillary electrophoresis is possible only if EOF is low and well controlled. A large EOF can sweep all of the analytes to the detector before they can be separated. Therefore, capillary surface needs to be modified to reduce EOF and to allow time for the separation to occur. In addition, the coating can often help to avoid unwanted nonspecific adsorption of analyte on the surface.

Adsorption of a basic analyte on the surface due to the electrostatic attraction between the surface and the analyte poses another challenge for improving the separation quality and efficiency. Of the various sources of band broadening – e.g. molecular diffusion, Joule heating and sample plug etc, the adsorption of the molecules on the surface is one of the most common sources. Adsorption causes peak tailing due to the retarded flow velocity of an analyte. Therefore, it is important to change the nature of the internal surface of capillary to a neutral or less negative or to a positive charge by applying a suitable coating material. In this regard, to prevent analyte adsorption and to reduce of the EOF, use of a capillary with dynamically coatings has been successful.<sup>4</sup> Consistent reduction of EOF creates reproducible migration times and is a vital component in CE separations.

One of the experimental objectives of this thesis was to estimate the effectiveness of several different coating techniques using silane-based surface modifying reagents such as, methoxypolyethylenoxysilane, cyclohexyltrimethoxysilane, and 3– methoxyacryloxypropyl trimethylethoxysilane along with a commercial polymer EoTrol LN<sup>®</sup>.<sup>5</sup> In order to compare the effectiveness of silane-based coatings inside the capillary, an experiment was performed to determine the migration times of fluorescent dyes –e.g. Rhodamine B (RhB) and Rhodamine6G<sup>+</sup> (Rh6G<sup>+</sup>) before and after coating. The fluorescent dyes have wide range of application including

fluorescent probes, fluorescence labels of nucleosides, nucleotides and nucleic acids and markers in electrophoretic techniques. The reasons for choosing these compounds are as follows 1) both of them have absorption maxima in visible range and 2) RhB is a neutral molecule. Hence it is not affected by applied electric field, but it flows along the EOF. However, Rh6G<sup>+</sup> migrates under the influence of the applied electric field so migration time of Rh6G<sup>+</sup> helps quantify electrophoretic mobility at specific electrolyte concentration, pH and nature of capillary wall coatings.<sup>6</sup>

In our experiment, the results of CE with RhB and Rh6G<sup>+</sup> with the coated capillaries showed that EoTrol LN<sup>®</sup> was more effective coating material at reducing the EOF than silane - based reagents. Hence applying EoTrol LN<sup>®</sup> dynamic coating, capillary isoelectric focusing (cIEF) was used to separate proteins and viruses. In cIEF, ampholytes, which is mixtures of amino acids, is used to create a pH gradient by applying electric field via electrodes dipped with an acid at one end and alkali at other end of capillary for cIEF separations.

Besides separation, the detection of analytes moving past the detection window is also a vital and challenging aspect in CE experiments. Detection is accomplished either by measuring analyte absorbance at its maximum wavelength under UV/VIS illumination or by measuring the fluorescent emission of a laser excited molecule. The detector sends an electrical signal to an analog-to-digital convertor card in the form of volts, and this voltage is received as data in a LabVIEW based data collection program in the computer. The data sent from the detector is processed into peak intensity versus time plot known as an electropherogram.

## 1.1 Principles of CE

### 1.1.1 Electrophoresis

Electrophoresis is a term to describe the phenomenon of charged particles to move with the differential velocity of in an electrolyte under the influence of an electric field.<sup>7</sup> The velocity of the particles in a fluid in the presence of electric field depends on their electrophoretic mobilities. The electrophoretic mobility of an analyte is a function of its size, charge, and the strength of electric field applied.<sup>8</sup> Electrophoresis was first observed in 1930 and was developed as a separation technique for colloidal particles in 1937 by Arne Tiselius. Since then, electrophoresis has gained widespread popularity and has evolved into different forms such as capillary zone electrophoresis (CZE), micellar electrokinetic chromatography (MEKC),<sup>9</sup> capillary isoelectric focusing (cIEF), isotachopheresis (ITP) and polyacrylamide gel electrophoresis (PAGE) etc. The use of denaturing agents such as sodium dodecyl sulfate (SDS) in PAGE was introduced in 1969 by Weber and Osborn resulted in another mode of separation - SDS PAGE – which is extensively used for separation of molecules in bio-technology. Electrophoresis in a capillary was first demonstrated in 1981 by Jorgenson and Lukacs.<sup>10</sup> Then capillary array electrophoresis was developed for DNA sequencing in 1990. Fully automated capillary electrophoresis instruments became available only after 1999.

Moreover, to explain differential velocity of analytes in buffer solution in electrophoretic separations, all the forces acting on a particle is to be considered. At steady state, the viscous drag force and the pull due to the electric field acting on a charged analyte counter act each other so there is no net force acting to accelerate the analyte. Therefore, the ion migrates towards the cathode with a constant velocity called the electrophoretic velocity.



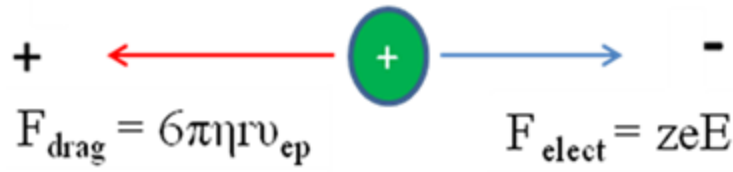


**Fig 1.1: Forces acting on a particle in fluid flowing under the influence of electric field**

Since  $F_{\text{net}} = 0,$  E.1

Rearranging E.1, we get  $U_{ep} = \frac{ze}{6\pi\eta} \frac{E}{r}$  E.2

$U_{ep} = \mu_{ep}E$  E.3

The electrophoretic velocity only depends on the charge, radius, and viscosity of the medium and the strength of applied electric field. However, in any electrophoresis experiment, the net electrokinetic velocity of the particle in a fluid is the sum of both the electroosmotic and electrophoretic velocities. The electroosmotic velocity is the flow of the buffer solution as a response to the applied electric field. If the ion in the buffer is negatively charged, movement of the ion is in the direction opposite of EOF. Electrokinetic velocity of negatively charged ion is less than the EOF velocity, but for positively charged ions, the electrokinetic velocity is greater than the EOF because the electrophoretic velocity is in the same direction as EOF. Neutral particles are not affected by the applied electric field so they flow with the velocity of the EOF as illustrated in Fig 1.2

$$U_{ek} = U_{eo} + U_{ep} \quad \text{E.4}$$

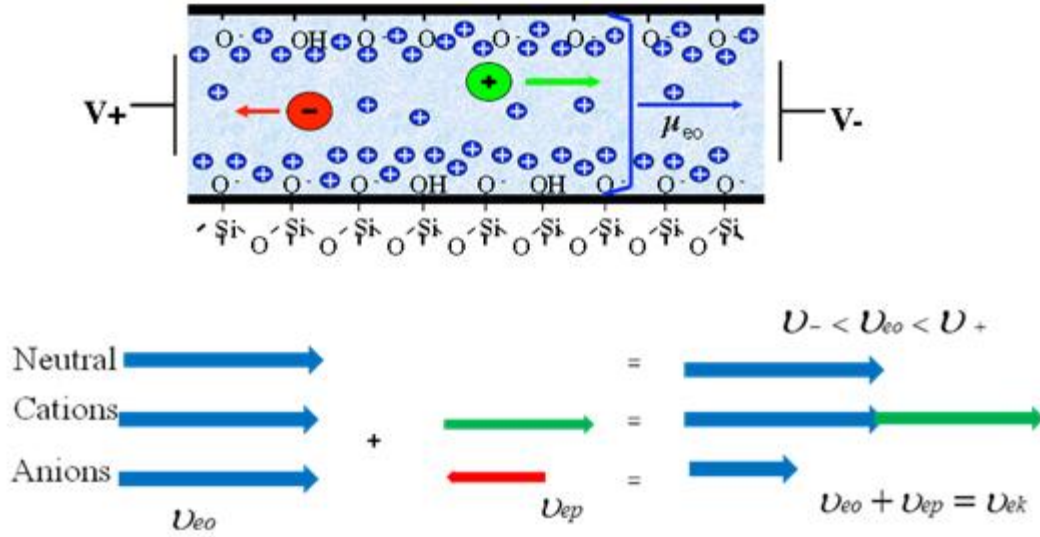


**Fig 1.2: Schematic of electrophoretic ( $v_{ep}$ ), electroosmotic flow ( $v_{eo}$ ) and electrokinetic velocity ( $v_{ek}$ ) of positive and negatively charged ion due to effect of applied electric field on ions.**

The electrophoretic mobility ( $\mu_{ep}$ ) of an ion as shown in E.3 is a proportionality constant that relates the electrophoretic velocity to the strength of applied field ( $E$ ) which subsequently depends on charge ( $ze$ ), radius ( $r$ ) and viscosity of the electrolyte medium as in E.5 .

Rearranging E.2,

$$\frac{v_{ep}}{E} = \frac{ze}{6\pi\eta r} = \mu_{ep} \quad \text{E.5}$$

For ions, electrokinetic mobility is equal to the sum of electrophoretic mobility and electroosmotic mobility.

$$\text{Therefore, } \mu_{eo} + \mu_{ep} = \mu_{ek} \quad \text{E.6}$$

Hence, analytes are detected in the detector in the order of decreasing electrokinetic mobility; cations, neutral and anions.

### 1.1.2 Electroosmosis

Electroosmosis is the motion of buffer induced by an applied potential across a porous material, capillary tube, membrane, micro channel or any other fluid conduit. This motion is the result of the formation of an electrical double layer (EDL) at the interface between the material and fluid due to the charged capillary surface. The EDL model describes the ionic environment in the vicinity of charged surface. Therefore, it is important to understand how EDL is formed at the interface between the fluid and other materials like fused silica, glass and metals. As illustrated in Fig 1.3, when the negatively charged surface comes in contact with buffer, the first inner most layer of cations adjacent to the surface is formed and remains immobile due to strong electrostatic attraction from the surface to cations. Therefore, this inner most layer is known as the compact, Inner Helmholtz (IHL) or stern layer. The IHL partially neutralizes the charge on the surface. In order to neutralize the residual negative charge, solvated cations from the bulk solution are attracted towards the surface. The second more diffuse layer consisting of solvated and mobile ions. This diffused layer is known as Outer Helmholtz (OHL) or diffuse layer.

Capillary is made up of the fused silica. Therefore, its surface is covered with silanol groups. There are approximately 4 to 5 silanol groups/nm<sup>2</sup> on smooth, nonporous, heat stabilized amorphous silica surface despite theoretical calculated for number of silanol group 7.8/nm<sup>2</sup>.<sup>12</sup> Despite some structural variation, surface silanol groups ionize in aqueous solution generating a negative charge on the surface.<sup>13</sup>



This double layer formation on the silica surface results in an electrokinetic potential distribution between the surface and any point in the bulk liquid.<sup>14</sup> This potential difference is on the order of millivolts and is referred to as the surface potential.<sup>14</sup> The magnitude of the surface potential is

related to the magnitude of surface charge and the thickness of the double layer. The potential drops off roughly linearly in the Stern layer and then exponentially through the diffuse layer. The potential curve as shown by bold red line in Fig1.3 is useful to show the distribution of potential across the EDL and to the bulk of the solution as a function of distance from surface. The boundary between the two layers, IHP and OHP, is called the slip plane and is usually defined at the point where the Stern layer and the diffuse layer meet. The potential difference between this point and bulk is called zeta potential. The zeta potential and EDL thickness both depends on ionic strength and surface charge in the solution. Fig 1.3 illustrates the formation of double layers and a plane in the double layer where the zeta potential ( $\xi$ ) is defined

If an electric field is applied across the capillary, excess solvated cations in diffuse part of double layer in the electrolyte are attracted to the negative electrode and drag bulk electrolyte with them resulting in a bulk fluid flow toward cathode. This pumping action is known as electroosmotic flow (EOF) and is shown in Fig 1.4. The velocity of the electroosmotic flow (EOF) is proportional to the strength of the applied electric field (E). Mathematically

$$v_{eo} \propto E \quad \text{or} \quad v_{eo} = \mu_{eo} E \quad \text{E.7}$$

where,  $\mu_{eo}$  is the proportionality constant between the fluid velocity and the applied field. This constant of proportionality  $\mu_{eo}$  is known as the electroosmotic mobility. Electroosmotic mobility depends on the dielectric constant of the fluid medium ( $\epsilon$ ), the zeta potential ( $\xi$ ) of the surface and the viscosity ( $\eta$ ) of the fluid as given in E.8

$$\mu_{eo} = \frac{\epsilon \xi}{4\pi\eta} \quad \text{E.8}$$

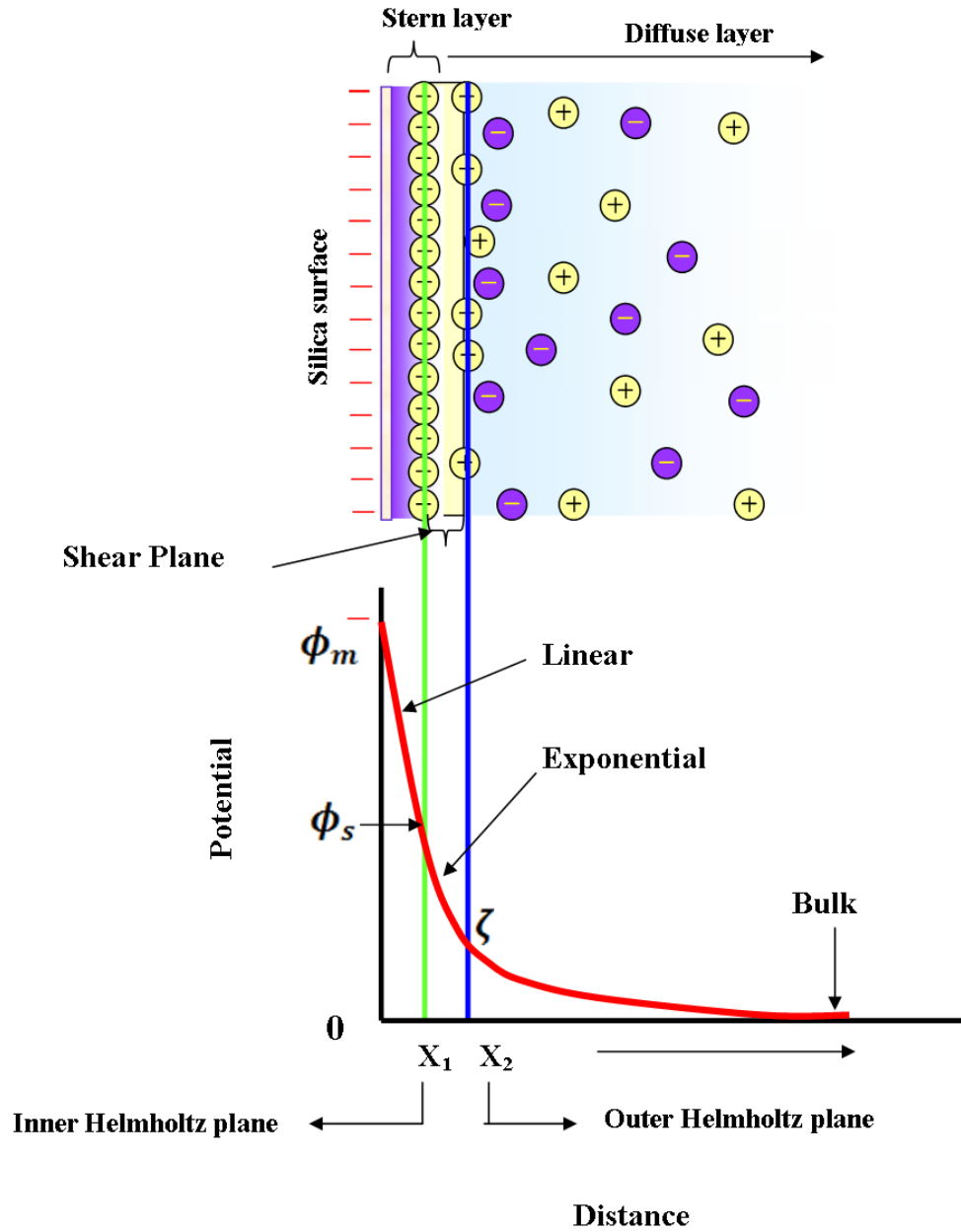


**Fig 1.3: Schematics of an electrical double layer formation on silica surface and a potential variation in double layer.**<sup>15,16</sup>

At low pHs, zeta potential is expected to decrease because of the recombination of  $\text{SiO}^-$  with excess  $\text{H}^+$  ions and at the higher ionic strength due to the partial collapse of the electrical double layer. Therefore at lower pH, EOF is relatively low.

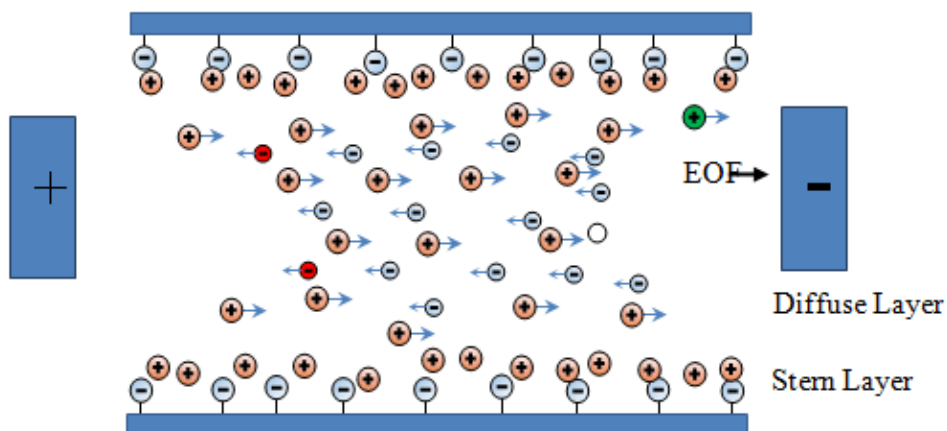


**Fig 1.4: Illustration of electroosmosis due to application of electric field in a capillary.**<sup>17</sup>

For capillary electrophoresis experiments, often times surface modifying reagents are applied intentionally in order to manipulate the EOF depending upon the nature and charge on the analytes. For example in Deoxyribonucleic Acid (DNA) separations, negatively charged DNA flows toward the positive electrode. If high electric fields are used, the EOF will be strong and the DNA molecules migrate in the opposite direction of the EOF. Generally EOF is much greater than the EP of the analyte.<sup>18</sup> Therefore either DNA does not separate effectively. Therefore surface of a capillary needs coatings 1) to prevent analyte-wall interactions that result in the adsorption on the surface, and 2) to devise effective and rapid separation method specific to analyte by using controlled EOF.<sup>19</sup> Ideally capillary surface coatings are stable under the separation conditions necessary for a successful separation, and preferably over a wide range of pHs. Therefore capillary surface are either temporarily coated with dynamic coatings or permanently forming Si-C or Si-O-C covalent bond on the silica surface. The mechanism of coatings is discussed in greater detail later in a separation section.

### 1.1.3 Separation Efficiency

Separation efficiency is a common way of reporting the quality of a separation. It is either expressed in terms of the number of plates (N) or plate height (H). Greater separation efficiency is indicated by a smaller theoretical plate height or the greater number of plates. These two terms are related by the following relation where L is the length of separation column:

$$N = \frac{L}{H} \quad \text{E.9}$$

In CE, efficiency of separation can be calculated by using following relationship:

$$N = \frac{L^2}{\sigma_{total}^2} \quad \text{E.10}$$

where L is separation length of the capillary and  $\sigma_{tot}^2$  is the total variance due to various sources of band broadening in the capillary. The efficiency of the CE system can also be derived from migration velocity.

$$v_{ep} = \mu_{ep} E = \mu_{ep} \frac{V}{L} \quad \text{E.11}$$

Migration time is defined as

$$t = \frac{L}{v_{ep}} = \frac{L^2}{\mu_{ep} V} \quad \text{E.12}$$

During analyte migration, molecular diffusion occurs as the analyte migrates through the capillary leading to band broadening. The band broadening ( $\sigma^2$ ) can be calculated by the following relation assuming that diffusion is the only major source of band broadening:

$$\sigma^2 = 2Dt \quad \text{E.13}$$

where D is the molecular diffusion, t is migration time. Band broadening due to molecular diffusion is explained in greater in the following sections elsewhere.

### 1.1.4 Resolution in CE

The resolution between two bands is a measure of the ability of a separation system to resolve two components and categorize overlap between adjacent peaks. If there are two component bands migrating down a separation channel, the resolution  $R_s$ , between the two zones is the difference in their positions divided by the average width of the peaks,

$$R_s = \frac{\Delta L}{4\sigma} \quad \text{E.14}$$

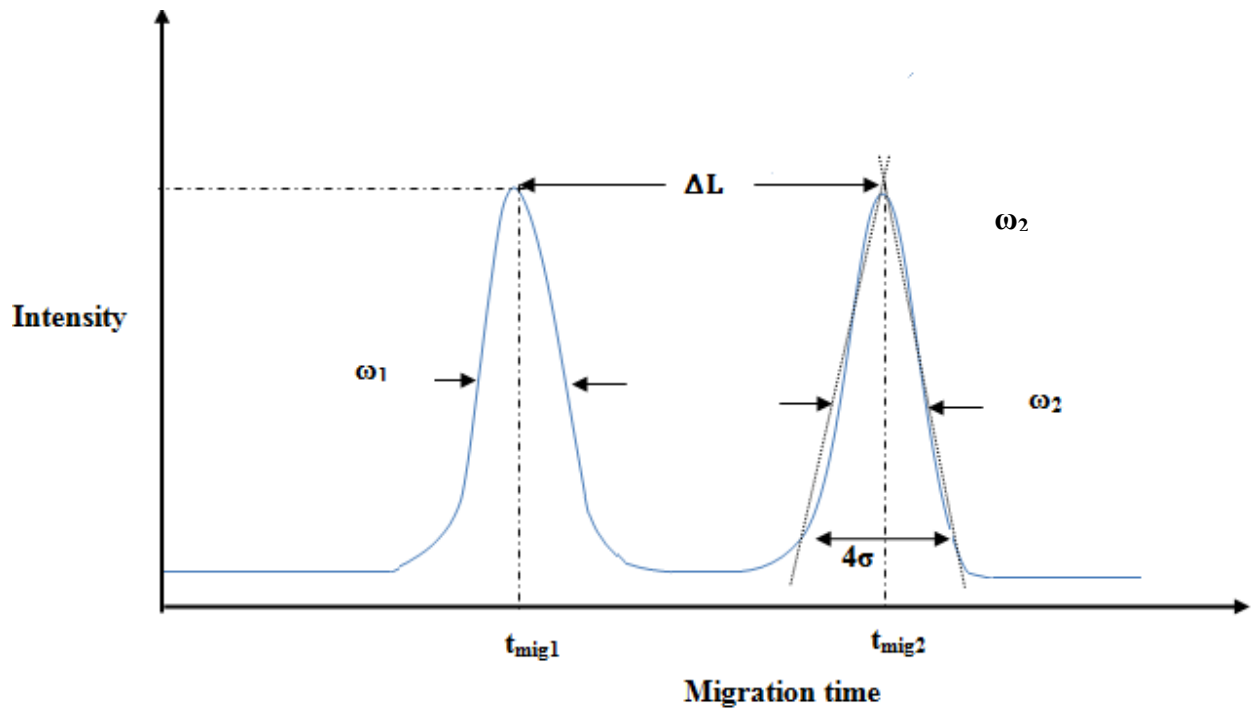


**Fig 1.5: Illustration of resolution of a peak, peak width at half maxima and base line width**

where  $L$  is the separation distance for components 1 and 2, and  $w$  is the width of the peak of components 1 and 2. The resolution between two species 1, 2 is also given by the following expression.

$$R_s = \frac{\sqrt{N}}{4} \left( \frac{\Delta\mu_{1,2}}{\mu_{1,2} + \mu_{eo}} \right) \quad \text{E.15}$$



where  $\mu_{1,2}$  and  $\Delta\mu_{1,2}$  are the average and the difference of the electrophoretic mobilities of two species 1 and 2 respectively. From E.15, it is obvious that the presence of the electroosmotic flow degrades the resolution and in some cases the electroosmotic flow can be best optimized to improve the resolution of a separation.

Increasing the voltage applied is a limited means of improving resolution. The practical limit of maximum voltage we can apply is 30 kV. By shortening the length of the capillary, field strength can be increased but it will again cause Joule heating. Therefore, the key to get high resolution is to increase ( $\Delta\mu$ ) the difference of electrophoretic mobility of analytes. The resolution can also be calculated by the migration analyte migration times and width of peaks at half height by the following relation:

$$R_s = 1.18 \left( \frac{t_{mig2} - t_{mig1}}{\omega_1 + \omega_2} \right) \quad \text{E.16}$$

where  $t_{mig1}$  and  $t_{mig2}$  are migration times of analyte 1 and 2 respectively and  $\omega_1$  and  $\omega_2$  are widths of peaks at half height.

### ***1.1.5 Advantages of CE***

Capillary electrophoresis (CE) is an efficient separation technique and performed using submicrometer volumes of sample in capillaries. The main advantages of CE are simple instrumentation, a wide selection of species that can be analyzed, a flat plug flow profile, high sensitivity and high separation efficiency. Besides simplicity, rapid analysis, automation, ruggedness, different mechanisms for selectivity, and low cost are other advantages of CE. Moreover, CE requires smaller sample volumes and yet offers higher efficiency and greater resolving power than that of HPLC.

### ***1.1.6 Modes of sample Injections***

A small volume of sample injection in capillary is important to minimize high cost of reagents and to improve separation quality. Besides, sample plug injection in all runs must be consistent for reproducible separation results. Mainly, sample injection in CE can be performed by using two methods; electrokinetic injection and hydrodynamic injection. Both of these methods are described below.

#### ***1.1.6.1 Electrokinetic injection***

In an electrokinetic injection, the capillary and the anode are simultaneously inserted into a sample vial keeping the cathode in the buffer reservoir at the other end of the capillary at the same height. A controlled voltage of about 5 kV DC is then applied across the capillary via the electrodes for 5 s to 20 s. After the injection is made, the capillary end and the anode are switched into the buffer vial and a high voltage of 20 to 30 kV DC is applied for enough time for separation to occur. Moles of sample injected by this method are calculated by the following formula as in E.17.

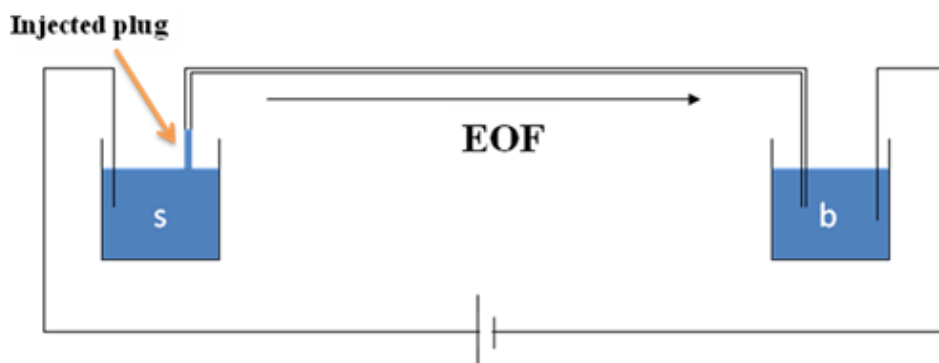


**Fig 1.6: Illustration of electrokinetic Injection of sample into a capillary for CE.**

$$\text{Moles of sample injected} \quad (n) = \mu_{ek} \left( E \frac{K_b}{K_s} \right) t \pi r^2 \quad \text{E.17}$$

Where  $\mu_{ek}$  is the electrokinetic mobility of analytes, E is field strength,  $K_b$  and  $K_s$  are conductivity of buffer and sample respectively, t is time of injection, r is the radius of capillary. The disadvantage of this method is, since moles of analytes injected by this method depend upon the electrokinetic mobility sample which is different from the sample plug. Therefore sample plug might have same composition as that of the sample.

### ***1.1.6.2 Hydrodynamic sample injection***

An alternate method of sample injection into the capillary is the application of hydrodynamic pressure. In this method, either the sample is introduced into the capillary using a syringe, using a vacuum pump or by lifting the sample vial to a certain height for a few seconds. The following E.18 is used to calculate the volume of the sample injected by hydrodynamic methods.

$$\text{Volume} = \frac{\Delta P \pi d^4 t}{128 \eta L_{total}} \quad \text{E.18}$$

Where  $\Delta P$  is pressure difference between two ends of capillary, d is the diameter and  $L_{total}$  is the length of capillary, t is the time of injection, and  $\eta$  is the viscosity of the sample.

Between these two methods, the electrokinetic method of sample injection can be easily controlled to obtain a consistent volume of sample injection. But electrokinetic injection is injection biased, hydrodynamic injection with syringe pump is considered better because it is not biased and more reproducible sample plug.

## 1.2 Source of band broadening in cIEF

After the sample is injected into the separation capillary, the bandwidth of the peak representing an analyte is affected by several factors such as longitudinal diffusion, injection length, detection window, flow profile, Joule heating, electro-dispersion etc. The efficiency of a separation is expressed in terms of bandwidth which can be expressed in terms of the variance ( $\sigma^2$ ) of the concentration distribution of the band. All of the above mentioned sources of band broadening may or may not be operative in CE depending on the mode and the conditions set up for a particular separation. Most of the sources of band broadening mentioned above operate independently under a specific set of experimental conditions, so the variances caused by them are additive in nature. The total variance,  $\sigma_{total}^2$  can be written as:

$$\sigma_{total}^2 = \sigma_{diff}^2 + \sigma_{inj}^2 + \sigma_{det f}^2 + \sigma_{joule}^2 + \sigma_{ads}^2 + \sigma_{edisp}^2 + \sigma_{flow}^2 \quad E.19$$

Except under extreme operating conditions, such as a high voltage or high conductivity, most of the bands broadening factors are insignificant. In order to get consistent results in CE, there are several parameters to be optimized which can cause band broadening. The different sources of band broadening will be discussed more thoroughly in the following sections. Slight changes in sample plug length, run voltage, detection window size, capillary length, composition of run buffer and the type of coating material can result in a significant negative impact on the reproducibility of migration time and separation efficiency (N). The following sections describe more thoroughly the mains sources of band broadening in CE.

### 1.2.1 Molecular diffusion

In HPLC there are four general contributions to broadening due to chromatographic columns. These are known as: 1) eddy diffusion, 2) longitudinal diffusion, 3) mass transport broadening in the stationary phase, and 4) mass transport broadening in the mobile phase. In CE, as there is no packed column for mobile phase to flow through, peak broadening due to eddy diffusion is zero. As there is no stationary phase, the mass transport in the stationary phase can be eliminated from the van Deemter equation E.20.

$$H = A + \frac{B}{\nu} + C\nu \quad \text{E.20}$$

Since  $A = 0$  and  $C = 0$ ,  $H = \frac{B}{\nu}$  E.21

Where H, A, B and C represent height equivalent to theoretical plate (m), band broadening to eddy diffusion (m), longitudinal diffusion ( $\text{m}^2/\text{s}$ ) and mass transfer term (unit less).

Hence, efficiency of CE separation only determined by flow velocity and longitudinal diffusion term B because fluid flow is laminar in micro scale dimension capillary. It should be remembered that the smaller the reduced plate height (H) the better. At high flow rates ( $\nu$ ),  $B/\nu$  term becomes smaller and hence H gets smaller. The smaller the plate height, the more efficient is the separation. Hence the contribution of longitudinal diffusion to peak broadening is smaller. Diffusion is also described in one dimension using the Einstein–Smoluchowski E.22.

$$\sigma^2 = 2Dt \quad \text{E.22}$$

where  $\sigma^2$ , D, and t are the variance, diffusion coefficient and migration time, respectively. Sigma ( $\sigma$ ) can be considered the distance moved by a particle or molecule over the time period t.

### ***1.2.2 Adsorption on surface***

Adsorption of samples on the surface of the capillary leads to tailing the analyte bands. Sometimes, the capillary becomes clogged and might be rendered useless due to excessive adsorption. Basic proteins are positively charged at neutral pH, so they can be adsorbed on the negatively charged capillary surface. Therefore, the capillary surface needs to be modified to decrease the negative charge by applying a coating on the surface before injecting the sample.

### ***1.2.3 Effects of voltage and temperature***

Both the electroosmotic and electrophoretic velocities are directly proportional to the field strength. But increasing the voltage does not always increase the separation efficiency because it also increases EOF. Higher EOF sometimes results in inefficient separation because the high EOF sweeps all analytes too quickly across the detection window without allowing time for a separation to occur. Therefore, low EOF is often desired even in the case high field strength is applied. The most important limiting factor for applying higher voltage is Joule heating. Joule heating occurs due to the voltage drop in the solution as the current flows through the motion of ions toward the electrodes of opposite charges. In other words, Joule heating arises due to the dissipation of the applied electrical power (P) when the current (I) passes through the electrolyte with a resistance (R) in the capillary. The current increases as the applied voltage increases.

$$P = IV = I^2 R \qquad \text{E.23}$$

Experimentally, the optimal voltage is determined by performing runs at increasing voltages until deterioration in resolution is noted. The electrophoretic mobility and the electroosmotic flow expressions both contain a viscosity term in the denominator. Viscosity is a function of temperature; therefore, precise temperature control is important. As the temperature

increases, the viscosity decreases; as a result, the electrophoretic mobility increases. Besides a decrease in viscosity, excessive Joule heating may cause the buffer solution to boil. In the case where the buffer boils, the capillary fills with bubbles that can be indicated either by a sudden drop or by a rapid fluctuation in current in the capillary. The main problem that is often encountered during microchip or capillary electrophoresis separations are the formation of bubbles inside the capillary due to excessive Joule heating. To minimize Joule heating, low concentration buffers like 20 mM are often chosen. Low ionic strength buffers decrease the current. Longer and smaller diameter of channels has large surface areas, generate less heat and dissipate heat generated inside the capillary more rapidly. Some buffers are more pH-sensitive with temperature e.g. Tris buffers. In a complex separation involving many proteins and peptides in the mixture, even a small pH shift can alter the selectivity.

#### ***1.2.4 Detection-window band broadening***

Many organic compounds absorb in the UV or visible (Vis) region of electromagnetic spectrum. The color absorbed and transmitted are complimentary to each other in visible region. Proteins, including those in tissues, and peptides absorb ultraviolet (UV) light quite strongly. It is the amino acids that make up the proteins that absorb the UV light. The label free detection and characterization of the proteins by absorption spectroscopy and infrared spectroscopy became feasible because of the strong absorbance by the most proteins in the UV region. Capillaries consist of quartz glass which allows UV light to pass through and hence allows the detection of proteins by absorbance measurement. The optical absorbance of proteins is usually measured at 280 nm. At this wavelength, protein absorbance is mainly due to the amino acids; tryptophan, tyrosine, and phenylalanine with their molar absorption coefficients decreasing in that

order.<sup>20</sup> The peptide bonds found in the amino acids also absorb at 205 nm. Of course, the molar absorption coefficient of the protein itself at 280 nm will depend upon the relative concentrations of these three amino acids. Therefore, different proteins can have different absorption coefficients and even the wavelength of the maximum absorbance may differ. The UV absorbance of a protein can be used both to quickly image and acquire spectra of microscopic samples non-destructively. The spectra can also be used to determine protein concentrations and the relative amounts of protein to DNA or RNA. Absorbance measurements are governed by the Beer-Lambert law as in E.24

$$A = \epsilon bc \quad \text{E.24}$$

Where A is the absorbance which is the logarithm of ratio of the intensity of light transmitted to the intensity of the incident light,  $\epsilon$  is the molar absorptivity, and b is the path length of sample and c is the concentration of sample in the solution as shown in Fig.24. If the optical path length is cylindrical in shape, it causes more dispersion. Using of rectangular shaped capillary or channel minimizes dispersion due to diffraction from its surface.

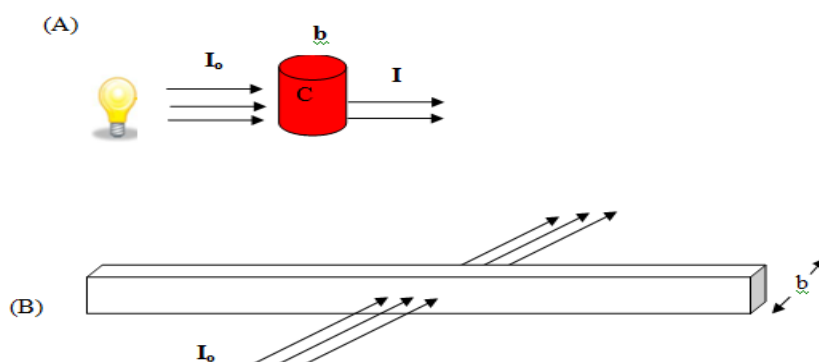


**Fig 1.7: Illustration of irradiation  $I_0$  of a sample on cylindrical optical path (A) and rectangular path (B) absorbance by a sample.<sup>21</sup>**



$$A = -\log \frac{I}{I_0} = -\log T$$

**E.25**

The path length in a CE capillary is 25  $\mu\text{m}$  to 75  $\mu\text{m}$  but in HPLC, the path length will be in several millimeters. Taking rectangular capillary instead of cylindrical can also minimize dispersion due to detection window. The following strategies can be adopted to improve UV/VIS

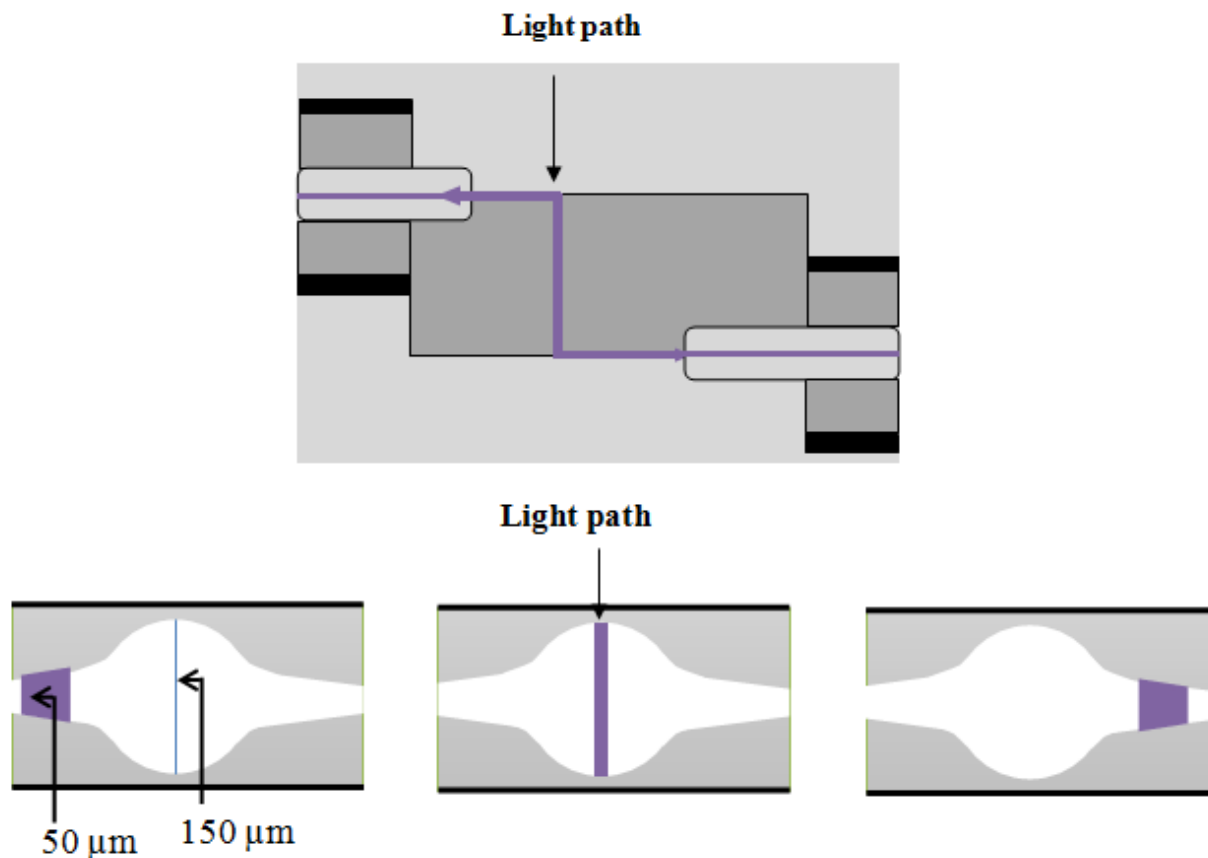


**Fig 1.8: Illustration of Z - cell (A) and bubble cell (B) for UV/VIS absorption detection sensitivity enhancement.**<sup>24</sup>

the sensitivity of detections – extended path length and sample stacking. An extended path length is created using a bubble cell or Z-cell.<sup>22</sup> Bubble cells enhance the UV/VIS sensitivity by factor of 3 to 5 where Z-cell can improve the signal to noise ratio by factor of ten but causes some band broadening.<sup>23</sup> In sample preconcentration and stacking, ionic strength of sample is much lower

than the run buffer. Since ionic conductivity in sample is much lower, ions move faster than in buffer therefore ions stack at the edge of sample zone. Stacking can improve signal to noise ratio 10 to 20 times.<sup>22</sup>

Detection of an analyte in CE by absorbance measurement is a universal method, though CE can be coupled with several other detection modes such as Laser-induced fluorescence (LIF)<sup>25</sup>, conductivity or amperometry<sup>26</sup> and mass spectrometry methods.<sup>27</sup> The following paragraphs highlights the advantages and disadvantages of absorption and LIF detection method.

An alternative but extremely sensitive detection method is Laser-Induced fluorescence (LIF). The detection limit of LIF is  $10^{-18}$  to  $10^{-20}$  moles whereas for absorbance detection of the smallest mass that can be detected is  $10^{-13}$  to  $10^{-14}$  moles. In absorbance detection, the sample is irradiated with light source either in UV range or visible range, an electron from an occupied molecular orbital is promoted to an unoccupied molecular orbital, in other words, the excited electron jumps from a highest occupied molecular orbital (HOMO) promoted to the lowest unoccupied molecular orbital (LUMO).

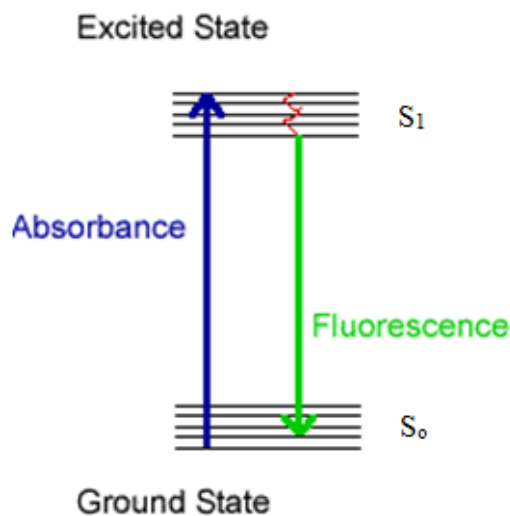


**Fig 1.9: Jablonski diagram to illustrate absorption and fluorescence phenomena in Laser induced Fluorescence detection method.**<sup>28</sup>

In LIF detection; high power narrow laser beam is used to excite the sample. After certain time of excitation, the energy absorbed by the sample molecules is emitted back in different wave length. This method of relaxation of an excited molecule is called fluorescence. Fluorescence can be best explained by Jablonski diagram Fig 1.9. Fluorescence detection method can be used in CE for samples that naturally fluoresce or are chemically modified to contain fluorescent tags. In both of these detection modes, the detection window length is generally defined either by the interrogation beam (laser beam) spot or the spatial filter aperture whichever is smaller. If the effective spatial filter aperture is smaller than 20 $\mu$ m, dispersion due to a spatial filter is insignificant and hence can be ignored.

### **1.3 Instrumentation**

One of the important features of CE is the simplicity of the instrumentation. Instrumentation for CE consists of 1) a high volt power supply capable of delivering  $\pm 30$  kV, 2) two electrolyte reservoirs, 3) a fused silica capillary filled with run buffer, 4) an on-column detector (UV/Vis absorbance detector), 5) two lamp sources, a deuterium lamp for UV and tungsten – halogen lamp for visible region, 6) a data storage and a processing device (DAQ card) and LabVIEW data collection software.

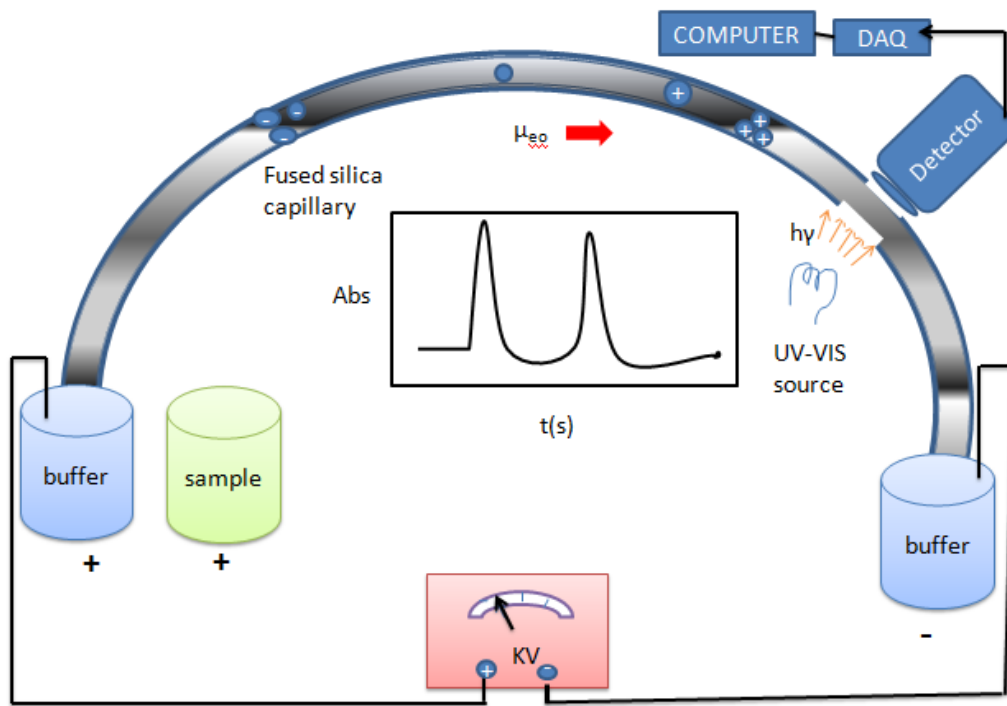


**Fig 1.10: Schematics of experimental setup for CE.**<sup>24</sup>

## 1.4 Modes of CE

Very often, CE is known as capillary zone electrophoresis (CZE) but there are other modes of CE including capillary gel electrophoresis (CGE), capillary isoelectric focusing (cIEF), capillary isotachopheresis (CITP) and micellar electrokinetic capillary chromatography (MECK). One similarity in all these modes of CE is that analytes migrate through electrolyte solutions under the influence of an electric field. A difference between CITP and CZE is that the sample injection is sandwiched between two different electrolytes; a leading electrolyte (high mobility) and trailing electrolyte (low mobility) solution. The sample components separate into bands according to the individual mobilities of the analytes only after the application of electric field. The electric current in the capillary is initially determined by the leading electrolyte, which

defines ionic concentration in the following band. The electric field strength varies in each band, with the highest strength found in the band with the lowest mobility ions. The current is same throughout run, each of the ionic bands move with the same velocity toward the detector.<sup>29</sup> There is not a buffer between the bands so band broadening due to diffusion is highly reduced in CIEF. But in cIEF analytes concentrate into bands according to their difference isoelectric point after certain time of application of electric field. The details of the working principle, procedures and the applications of cIEF will be discussed below.

### **1.5 Capillary Isoelectric Focusing (cIEF)**

cIEF is one mode of the several electrophoretic separation techniques in which proteins are separated on the basis of their isoelectric points (pIs). Isoelectric point is the pH at which proteins attain overall neutral charge. Isoelectric focusing (IEF) was first invented by Olof Vestberg and Torkel Wadstrom in 1967.<sup>30</sup> Later, with the development of capillary electrophoresis, IEF was successfully transferred to a capillary by Hjerten in 1985 from its slab gel based predecessor.<sup>31</sup> cIEF combines the high resolving power of conventional slab gel IEF with the advantages of simple CE instrumentation. A cIEF system typically includes a capillary with an I.D. 25  $\mu\text{m}$  to 200  $\mu\text{m}$ , a high voltage power supply, an online UV detector and a computer interface. There are three steps in cIEF, sample preparation, injection, isoelectric focusing and detection. When cIEF is conducted, the capillary is filled with the protein samples and carrier ampholytes. Then electrolytes are connected to the power supply by electrodes, while anode reservoir is filled with acidic and cathode reservoir is filled with alkaline solution. Upon application of electric field between anolyte and catholyte reservoirs a stable pH is formed by carrier ampholytes (CAs) and proteins are focused to their pI.<sup>32,33</sup> Focusing of analytes is

achieved rapidly (within few minutes) is accompanied by an exponential drop in the focusing current with constant applied voltage.

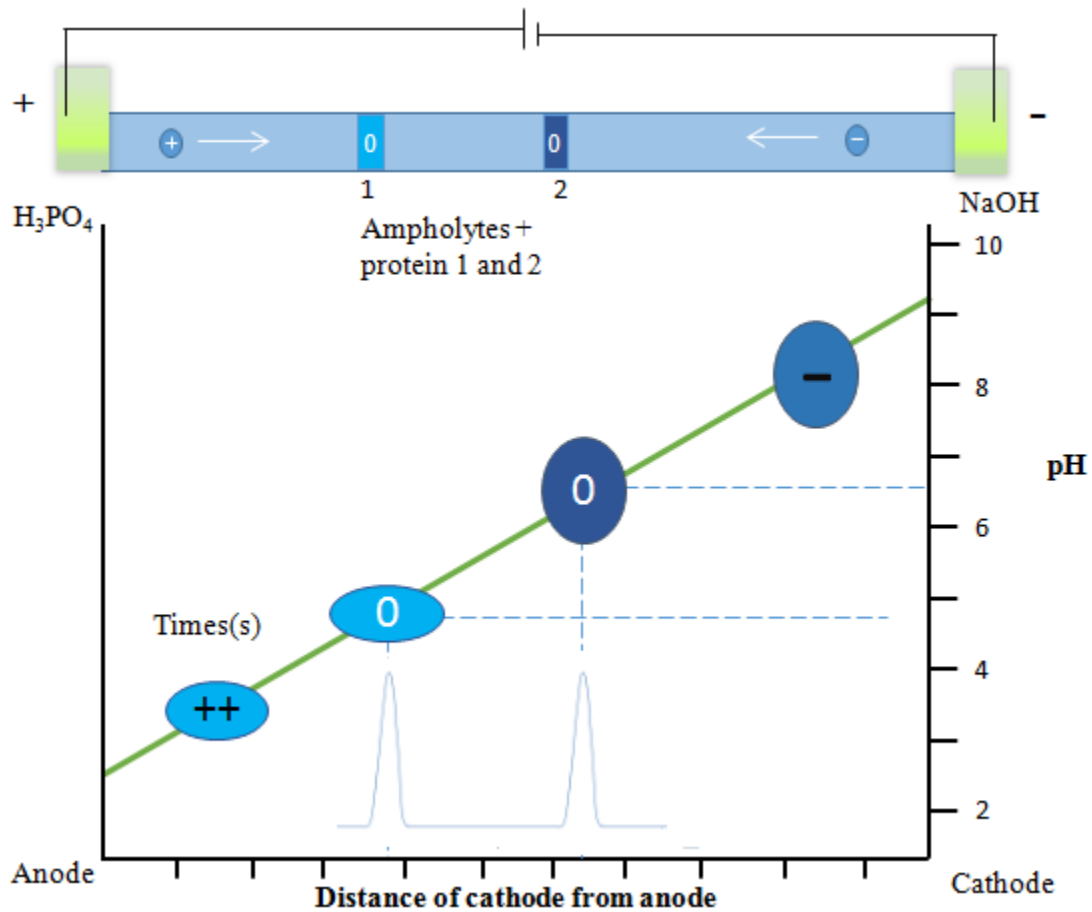


**Fig 1.11: Schematic of isoelectric focusing process. The proteins at pH higher than pI migrate towards anode but a protein at the pH lower than its pI move toward cathode until they attain overall zero net charge.**

A protein is positively charged if local environment pH below its pI and negatively charged if pH is above its pI. Thus at a pH below the pI, a protein migrates toward the cathode during electrophoresis and if pH is above, it migrates toward the anode. However, if a protein encounters an environment with pH equal to pI, it completely stops moving in either direction because mobility of the protein in the electric field depends upon its charge due to protonation

and deprotonation of amino and carboxylic groups. At steady state, electro-neutrality exist, it can be represented by the equation.<sup>32</sup>

$$C_{H^+} + \sum C_{NH_3^+} = C_{OH^-} + \sum C_{COO^-} \quad \text{E.26}$$

Where  $C_{H^+}$ ,  $C_{OH^-}$ ,  $C_{NH_3^+}$  and  $C_{COO^-}$  are concentrations of hydrogen ion, hydroxyl ion, sum of all positively charged amine and carboxylic ions respectively. If a protein at its pI were to migrate in pH gradient, the amino groups would need to be protonated again. Then the proteins become charged again and it starts moving towards the cathode. But as it moves along pH gradient to the cathode, it encounters high pH environment so the amino group will be deprotonated. As the proteins lose hydrogen ions, they become more negatively charged and are attracted towards anode. In this way, the proteins get focused and concentrated into sharp bands in the pH gradient at its characteristic pI. In order to detect proteins in cIEF, the focused bands need to be either moved or online single point detection or whole length of the capillary need be scanned. The methods of detection for cIEF are described separately in later sections

### ***1.5.1 Establishing pH gradient***

The key to success in gel IEF or cIEF depends on the creation of linear and stable pH gradient in the electric field. The pH gradient can be established in two ways; using carrier ampholytes and acrylamido buffers. The carrier ampholytes are mixtures of high number of synthetic amphoteric molecules containing poly amino and poly carboxylic acid groups. The pH range of CAs can be selected wide range (e.g. pH 2 to 11) are commonly used to separate protein samples with widely different pI or estimate of an unknown protein. Narrow pH of CAs (6-8) is used to get high resolution separation of closely related amphoteric species. Final concentration of 1% CAs is commonly used in gel IEF and concentration of 4% CAs. In the electric field, the ampholytes partition into a smooth pH gradient between the anolyte and the catholyte. Recently

some attempts have been made to create CAs free gradient such as temperature gradient buffer filled capillary or using a continuously tapered capillary but separation resolution has been compromised.<sup>34</sup>

### ***1.5.2 Carrier Ampholytes***

Carrier Ampholytes (CAs) is a mixture of 600 to 700 synthetic chemicals (a series of polyamino, polycarboxylic acids or polyamine – polysulphonic acids groups) that possess slightly different pI over a selected pH range are essential for IEF to achieve high resolution separation. Ideally, these molecules are water soluble, have certain buffer capacity in their isoelectric state, have a certain conductivity to contribute to the current, have low absorbance at 270 nm or higher to facilitate absorbance detection and be without any hydrophobic group to prevent possible interaction with analytes. The compositions CAs from different manufactures vary due to different syntheses used. Ampholine® which is produced by reacting aliphatic oligoamines with acrylic acids. Another ampholyte is Pharmalyte® pH 3 to 10 which is copolymer of glycine, glyglycine, amines and epichloroethrin. Therefore, mixing ampholytes with multiple vendors will increase resolution due to increased number of CAs' present in a particular range. The quality of separation in cIEF mainly depends on the pH gradient or quality of ampholytes.<sup>35</sup> The narrower pH gradient, the better would be the resolution but it limits wider application for the separation of various proteins and peptides. General properties of amino acid proteins are discussed in the following section.



### ***1.5.3 Amino acids and proteins***

Proteins are large biological molecules or macromolecules consisting of one or more polypeptide chains of amino acid residues. Therefore, amino acids are known as building block proteins. Proteins perform a vast array of functions within living organism, including catalyzing metabolism, replicating DNA to stimuli, and transporting molecules from one location to another etc.<sup>11</sup> Proteins differ from one another primarily in their sequence of amino. A protein, a peptide and an amino acid are amphoteric because they all contain carboxylic groups (-COOH) terminal and amino groups (-NH<sub>2</sub>) terminal. Therefore, each amino acid has at least two pK<sub>a</sub> values (some amino acids have more pK<sub>a</sub> values because they have additional acidic or basic groups). The presence of multiple acidic and basic groups in a single molecule enables the molecule to exist in several different charged states. As a simplest example, glycine can have a charge of +1, 0, or -1, depending on the pH of its environment. The two pK<sub>a</sub> values of glycine, pK<sub>1</sub> = 2.43 and pK<sub>2</sub> = 9.6 represents the equilibrium of protonation of amine group at low pH and deprotonation of carboxylic group at high pH. A careful titration of glycine against strong base like NaOH yields curve as in Fig 1.12. From the pK<sub>1</sub> and pK<sub>2</sub> values, pI of glycine can be calculated as  $pI = (pK_1 + pK_2)/2 = (2.43+9.6)/2 = 6.015$ . At this pH, the overall charge of zero is attained by glycine because the charge due to basic amine group equals acidic group in the same molecule in the equilibrium. This state of the molecule when it attains zero overall charge is called zwitterions. All amino acids form zwitterions at their pIs. For glycine, zwitterions are formed at pH 6.0, but histidine forms zwitterions at a pH of 7.8. Therefore its pI is 7.8. Like amino acids, the overall charge on a protein depends upon the number of amino and carboxylic groups and pH of the local environment. If the number of amino groups in a particular protein exceeds the number of carboxylic groups, its pI will be low and is classified as an acidic protein.

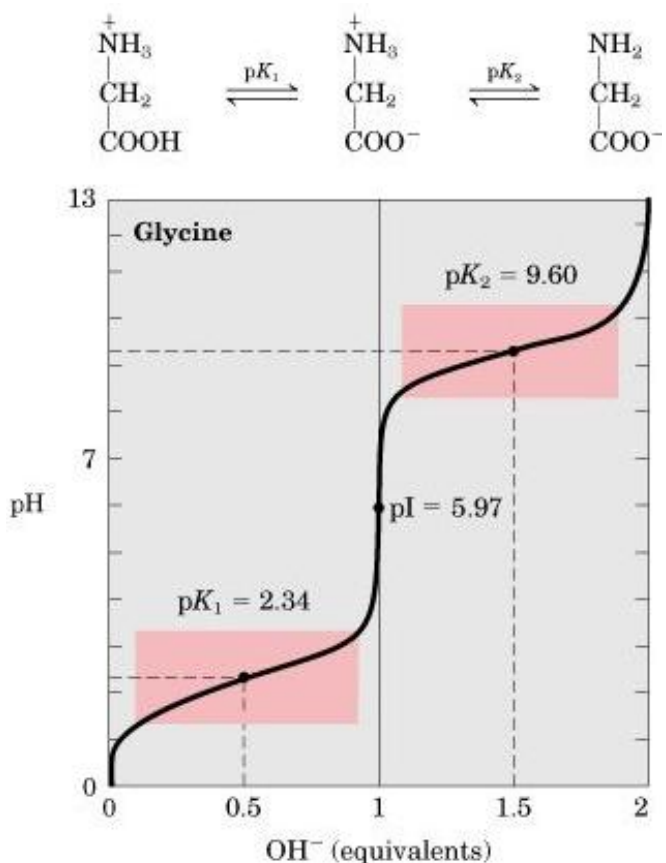


**Fig 1.12: Titration curve of glycine.<sup>21</sup>**

In the same way if the carboxylic groups outnumber the acidic group, the proteins is described as basic protein because its pI > 7. Proteins show considerable variation in their isoelectric points, between pH 3 to 12 with a great many having pIs between pH 4 to 7.

In cIEF, a mixture of polyamino, polycarboxylic acids is utilized to create a linear pH gradient in the electric field between acidic and basic solution. When a high voltage is applied via electrodes, all the amino acids migrate to the different regions to form a pH gradient between acidic and basic solutions at the ends. If a protein or a living microorganism is mixed with such an ampholytes mixture, it also gets focused in the certain region in the pH gradient in the presence of electric filed.

### 1.7.1 Resolution of cIEF

The resolving power in IEF is expressed in  $\Delta pI$  units' i.e. in the minimum difference of charge between two adjacent proteins that the IEF technique is able to resolve. Rilbe derived the following E.27 for minimally but definitely resolved zone.<sup>35</sup>

$$\Delta pI = 3 \sqrt{\left( \frac{D \left[ \frac{d^{pH}}{dx} \right]}{E \left[ \frac{-d\mu}{dpH} \right]} \right)} \quad \text{E.27}$$

E.27 illustrates that low diffusion coefficients (D), a high mobility slope  $d\mu/d$  (pH), high field strength (E) and a shallow pH gradient  $dpH/dx$  benefits in resolution. But E cannot be increased infinitely as it causes more Joule heating. The term diffusion coefficient D used in the E.27 is related with viscosity of the buffer by stokes law as in E.28

$$D = RT / \eta f \quad \text{E.28}$$

where  $\eta$  is the viscosity of the medium, R is the gas constant, T is the temperature in K,  $f$  is the frictional force ( $f$ ) =  $6\pi\eta r$ , where  $r$  is the radius of the molecule. By increasing viscosity of medium reduces D and hence improves the resolution as given in E.27. However, it decreases the efficiency causing the decrease in mobility slope  $d\mu/dpH$ . So the maximum resolving power demonstrated in a conventional IEF is 0.01 and but IEF in an immobilized polyacrylamide gel (IPG), the resolving power have demonstrated as low as 0.001 pH units.<sup>36</sup> However, cIEF can only separate a mixture of proteins whose pI value differs by 0.02 pH.

## 1.6 Detection

Detection in cIEF requires mobilization of inherently neutral species in the form of focused bands to an online single point or movement of the detector along length of capillary. Four methods have been developed for detection of focused zones. 1) on column single point detection by measuring absorbance using a UV-detector,<sup>20,37</sup> 2) whole column detection by measuring fluorescence using CCD camera,<sup>25,38</sup> 3) detecting chemiluminescence,<sup>39</sup> 4) mass spectrometric detection coupling cIEF with mass spectrometer.<sup>20,40</sup> The most common methods of detection, on column single point detection and whole column detection without mobilization of band, have been explained in the following section.

### *1.8.1 On-column single point detection.*

Commercial CE instruments use on-column single point detection where UV detector optics are aligned and held fixed. Because of this, the focused bands need to be driven past the detection point either by a changing chemical composition of anolyte or catholyte or by applying pressure from either end of capillary.<sup>41</sup> Consequently, cIEF requires two steps, focusing and mobilization. The mobilization is an important step in overall performance and reproducibility of result of cIEF separation. Two types of UV detectors are commonly used ;1) variable-wavelength (sometimes called "spectrophotometric" detectors, and 2) photodiode array (sometimes simply called "diode array" detectors). The photodiode array UV detector consists of following components; 1) a light source, 2) monochromator, 3) slit, 4) sample container, 5) diode array light sensors, 6) signal processor and computer.

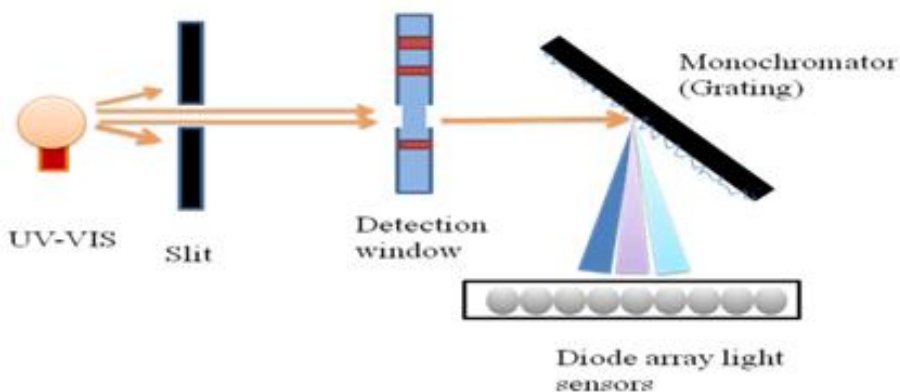


**Fig 1.13: Components of photodiode array detector.**<sup>24</sup>

The variable-wavelength detectors are less expensive; they are the standard detector type for quantitative analysis and routine assays. Photodiode array (PDA) detectors are more versatile, because they allow simultaneous acquisition of all wavelengths in real time. A schematic of PDA detector is given in Fig 1.13.

The on-column single point detector for cIEF requires a mobilization step which lengthens the analysis time and causes an uneven resolution along the separation channel. On-column single point detection can be used to detect the analytes labeled with fluorescent dyes. For example, detection of mitochondria have been demonstrated by fluorescent measurement at a single point using a probe 10-N-Nonyl acridine orange (NAO) separated by cIEF method.<sup>42</sup>

Chemiluminescence in CE has attracted much attention as a promising way to offer excellent analytical selectivity and sensitivity. Several reagents, such as luminal, acridinium, and peroxyoxalate have been utilized to create a photon emitted from a chemical reaction, which is also known as chemiluminescence.<sup>43</sup> A detector using luminal and H<sub>2</sub>O<sub>2</sub> chemiluminescence is considered simple and inexpensive experiment set up on pressure mobilization.<sup>44</sup> On column single point chemiluminescence detection of heme proteins has also been demonstrated in a glass

and glass/ PDMS microchip IEF. The principle of chemiluminescence reaction in this case is catalytic effects of heme proteins on reaction of luminal-H<sub>2</sub>O<sub>2</sub> enhanced by para-Iodophenol.<sup>45</sup>

### ***1.8.2 Whole column imaging detection***

Whole column imaging detection (WCID) was used for capillary isoelectric focusing for proteins and peptides by Qinglu Mao's group in 1999. A mixture of sample and ampholytes was introduced into a capillary, relatively short about 4 to 5 cm and an electric field applied to focus them. The focused zones were monitored in real time using an imaging detector. The concept of WCID is illustrated in Fig.1.14. Based on this conceptual model of imaging detection, three types of detectors have been reported including 1) refractive index gradient, 2) laser induced fluorescence (LIF)<sup>46</sup> and 3) UV absorption.

The mostly widely used whole column imaging detection method is absorbance. The whole column imaging detection eliminates the mobilization step required for single point on column detection after focusing is complete. Therefore, WCID technique not only speeds up analysis but it avoids the disadvantages associated with the mobilization process such as distortion of pH gradient and the loss of resolution. The whole column LIF detection provided a resolution of 0.03 pH unit. cIEF with whole column imaging detection has also been used for characterization and identification of human papillomavirus (HPV).<sup>46</sup> The pI of HPV was determined by cIEF – WCID.<sup>45</sup>

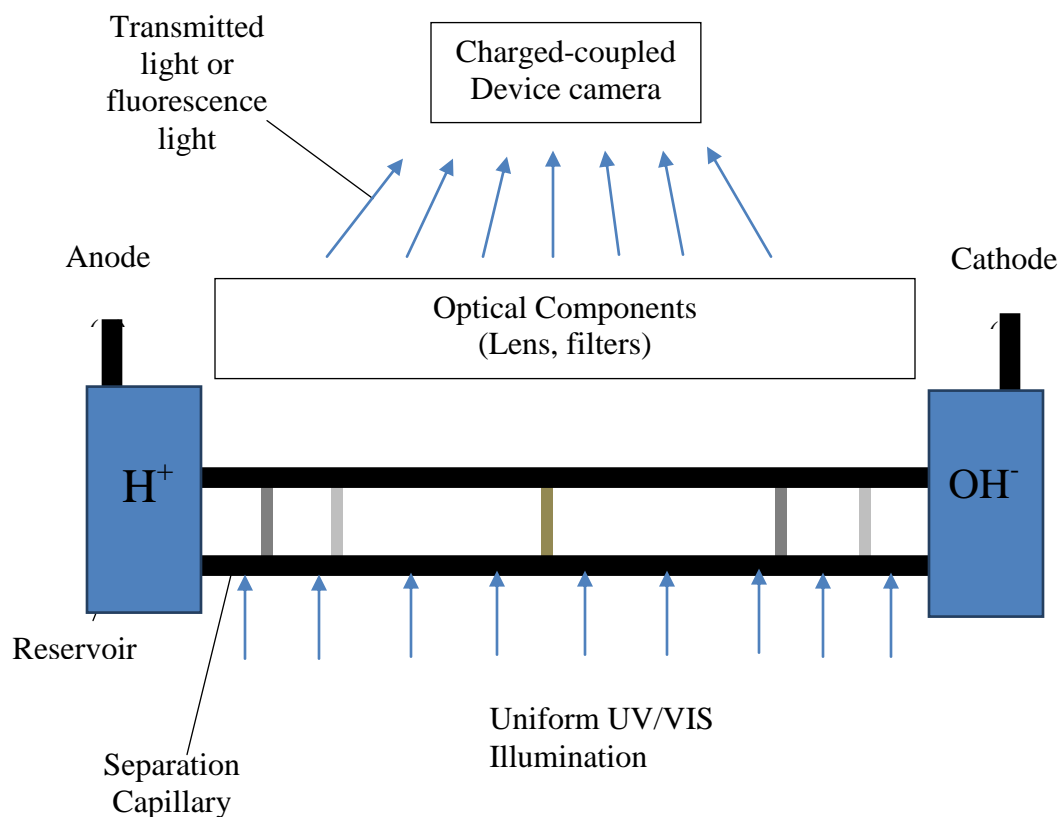


**Fig 1.14: An illustration of concept of Whole Column Imaging Detection (WCID) for cIEF separation.<sup>47</sup>**

### *1.8.3 Online cIEF- MS detection*

MS detection system can precisely measure the molecular mass of ions generated from the analyte. Mass spectrometry (MS) detection system can be coupled with CE through electron spray Ionization.<sup>48</sup> Generally, coupling of MS detection with CE has been accomplished using two different approaches; electron spray ionization (ESI) or a matrix assisted laser absorption/desorption mass spectrometry (MALDI). Both CE-ESI-MS<sup>49</sup> and CE-MALDI-MS provide excellent sensitivity and a wide mass range for analysis<sup>50</sup> though MALDI provide more flexibility than ESI-MS interfacing with CE.

## 1.7 Mobilization

Mainly, four band mobilization techniques have been developed for cIEF; 1) chemical mobilization, 2) hydrodynamic mobilization,<sup>51</sup> 3) gravitational mobilization,<sup>51</sup> 4) focusing and mobilization simultaneous.<sup>52</sup>

In chemical mobilization, either anolyte (0.02 M H<sub>3</sub>PO<sub>4</sub>) or catholyte (0.02 M NaOH) composition is changed by adding either a neutral or an acidic or a basic solution to alter pH so that separated proteins bands can migrate towards the detector.<sup>53</sup> Based on which catholyte or anolyte is replaced, the chemical mobilization can be divided into two types, namely anodic and cathodic mobilization.

### 1.7.1 Anodic mobilization

In anodic mobilization, the anolyte is replaced by a neutral salt such NaCl or Non proton cation solution. The main reason for adding a neutral salt is to raise ionic strength and pH of anolyte. When non proton cation (X<sup>+n</sup>) solution is added to anolyte, it gradually migrates into the capillary resulting in a progressive pH shift along the capillary. Then the ampholytes and the proteins molecules in focused bands become charged again. The condition of electro neutrality is now expressed as by E.29.

$$C_{X^{+n}} + C_{H^+} + \sum C_{NH_3^+} = C_{OH^-} + \sum C_{COO^-} \quad \text{E.29}$$

where  $C_{H^+}$ ,  $C_{OH^-}$ ,  $C_{NH_3^+}$ ,  $C_{COO^-}$ , and  $C_{X^{+n}}$  are concentrations of proton, hydroxyl ion,

positive, negative charged contributing groups and non-proton cationic solution respectively. The motion of H<sup>+</sup> toward the negative electrode makes the ampholytes and the proteins bands to be positively charged so the focused bands are mobilized to the detector. Therefore when application of the high voltage is resumed, the proteins bands are transported to detecting widow.



A schematic in Fig 1.15 illustrates the anodic mobilization by replacing anolyte with a neutral salt solution (NaCl). Movement of OH<sup>-</sup> toward anode helps bands remained focused.

Zwitterions have better performance due to less ionic activity. It causes less band broadening due to less Joule heating. But a care must be taken to choose zwitterions whose pI is higher than of anolyte but less than the pI of sample Protein.<sup>54</sup>

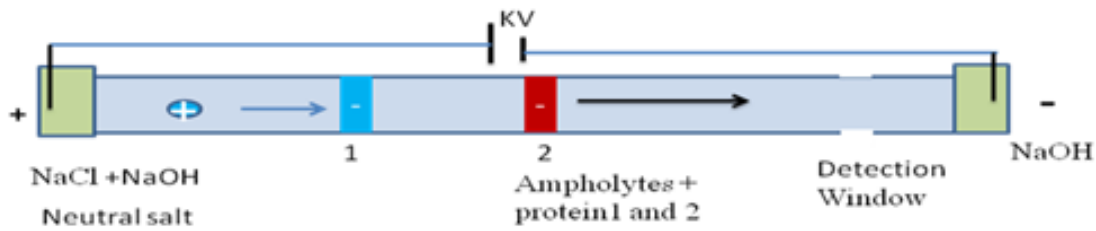


**Fig 1.15 : Schematics of anodic mobilization of focused proteins bands in cIEF.**

### ***1.7.2 Cathodic mobilization***

Cathodic mobilization is used for the acidic proteins having pIs < 5. For cathodic mobilization, a non - hydroxyl ion or with a neutral salt or an acetic acid solution is added in the catholyte. The equation of electro - neutrality is now expressed by the E.30. The weak organic acid such as acetic acid had a lower conductivity compared to the chloride and phosphate ions which were responsible for driving basic proteins toward the detector. The addition of migrating ions into the focused zone causes the pH to shift as the ampholytes must change to satisfy the electro-neutrality.

$$C_{H^+} + \sum C_{NH_3^+} = C_{OH^-} + \sum C_{COO^-} + C_{Y^{-m}} \quad \text{E.30}$$

where  $C_{Y^{-m}}$  is the concentration of non hydroxyl anion in the catholyte. The addition of non hydroxyl anion into catholyte leads to a decrease in pH along the capillary. This pH shift causes the proteins become charged again. If the high electric field is resumed, the protein bands are driven past the detector with the non hydroxyl anion. An illustrative diagram for cathodic mobilization is given in Fig 1.16.

Purified proteins and human plasma proteins have been separated by capillary isoelectric focusing and detected by cathodic mobilization, e.g. by replacing the catholyte solution (sodium hydroxide) solution by a solution containing another anion.<sup>55</sup> The effects of catholyte anions on the resolution of mobilized proteins were investigated. In comparison to chloride and phosphate, organic anions having small dissociation constants such as acetic acid demonstrated improved resolution in acidic proteins separation.<sup>55</sup>

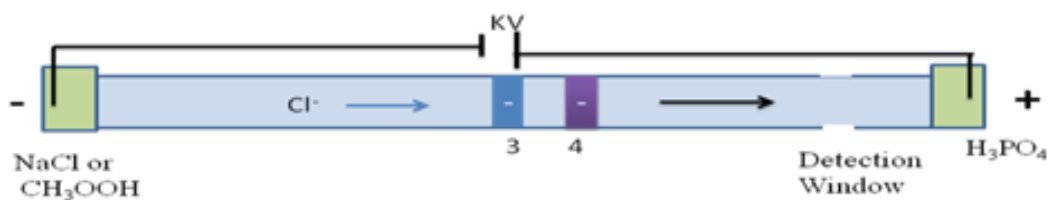


**Fig 1.16: Schematics of cathodic mobilization of separate protein band in cIEF.**

### ***1.7.3 Pressure mobilization***

Pressure mobilization utilizes either positive or negative pressure (usually either syringe pump or from vacuum pump).<sup>56</sup> The focused protein zones are forced to move toward the detector by applying pressure from one of the ends of the capillary. During pressure mobilization, it is necessary to continue applying electric field across the capillary in order to maintain the focused proteins zones intact.<sup>57</sup> The main disadvantage of pressure mobilization is the parabolic flow profile leading to band broadening and yielding poor

resolution. However, an advantage of pressure mobilization is greater mobilization efficiency and reproducibility compared to chemical mobilization.<sup>56</sup> Hjerten and Zhu's group have also demonstrated pressure mobilization by using compressed gas and by creating height difference.<sup>51</sup>

#### ***1.7.4 Advantages cIEF***

Though resolution of best slab gel IEF is around greater than traditional cIEF, (0.02 pH units), some of the advantages of cIEF include as follows: 1) cIEF takes shorter analysis time (within 10 to 20 minutes) than IEF in slab gel which usually takes several hours if not days to perform a complete analysis, 2) cIEF takes advantage of anti convective nature of smaller diameter (50 $\mu$ m) of the capillary which avoid unwanted mixing of analytes, 3) High Thermal conductivity of fused silica and large surface/volume ratio allows higher field strength, 4) Higher field strength allows shorter focusing time and better resolution, 5) Narrower diameter of capillary allows detection of pg quantity of material, 6) UV detection from clear silica capillary allows precise quantitative detection, 7) cIEF also provides greater opportunity for complete automation is a nondestructive analysis, 8) After the capillary surface is preconditioned, it maybe coated with a reagent not only to suppress EOF but to prevent adsorption of specific analytes on the surface. This will improve specificity, reproducibility, and provide high resolution similar to conventional IEF.

## 1.8 Capillary surface coating

Development of wall coating is an active area of research. Capillary wall coatings are described as static or dynamic based on the attachment of coating on the wall.<sup>19</sup> Static coatings involve covalent bonding between capillary walls and coating material while dynamic coatings involve just adsorptive secondary interactions.<sup>58</sup>

There are many reasons of chemical modification capillary wall in electrophoresis. Goal may include reduction or elimination of analyte-wall interactions, alteration of electroosmotic flow to effect more rapid separation, improved reproducibility or resolution of particularly difficult separation problems.<sup>59</sup> The hydrophobicity of coating is important factor. Strongly hydrophobic coatings are usually optimal for separation of bio-molecules, though other applications may require hydrophilic properties.<sup>60</sup>

Capillary and glass surfaces are hydrophilic in nature so polar molecules can easily be adsorbed. Basic proteins and the large bio-molecules such as polysaccharides etc will be adsorbed on the surface. So it is necessary to find a way to prevent the absorption of proteins on the surface and to reduce the EOF in CE. Surface modifying reagents MeOH, EtOH, ACN, silane-based reagents, polyvinyl alcohol (PVA),<sup>61</sup> and methyl cellulose, hydropropyl methyl (HPMC) and N substituted polyacrylamides<sup>36</sup> etc. have been widely used to change the capillary surface for CE experiments. Characterization of properties of capillary coating is extremely difficult because of small size and relatively inaccessibility of surface involved. Characterization of properties of surface coating is usually performed to measure EOF and to investigate its dependence on the pH of the buffer.

There are four main approaches to modify the capillary surface, including 1) controlling ionic strengths or pH of the electrolyte, 2) modifying surfaces by dynamic coating, a non-

covalent ways to get capillary coated, 3) modifying the capillary surface permanently by physical sorption, and 4) modifying the surface permanently with by covalent bonding.<sup>62</sup> The non-covalent coating and the covalent coating are discussed further in the following topics.

### ***1.8.1 Dynamic Coating***

Dynamic coating is an attractive coating as it overcomes difficulties of conducting reproducible and homogenous chemical derivatization in the capillary surface.<sup>4</sup> Dynamic coating is typically prepared by rinsing the capillary with a solution containing a coating agent that is either a polymer or a small molecular mass compound.<sup>58</sup> Because of the attachment of coating to the wall is based on the adsorption, a small amount of coating agent is usually added to the separation medium to keep the coating on the capillary wall surface.<sup>63</sup> The life time of dynamically coated capillaries can be extended by using an occasional simple regenerating process. Different types of polymeric and small molecular mass buffer additives are used as dynamic coatings for example poly(dimethylallylammonium chloride) (PDMAC), Polyethyleneimine (PEI), Polyarginine (PA), cellulose acetate, cellulose triacetate, Polyvinyl Chloride (PVC), Polyalkyl glycol(PAG), Polyethylene oxide(PEO).<sup>63</sup> Positively charged surface coating on capillary such as PDMAC, PEI, and PA which can effectively be used to separate proteins and peptides. Harvoth et al. demonstrated other neutral polymeric coating like PAG, PEO, and cellulose triacetate to reduce EOF and eliminate interaction between analyte and wall.<sup>19</sup> Physically adsorbed modification can be washed away by flushing with NaOH and methanol and then finally by deionized water then the same capillary becomes reusable for several days. The capillary being used for separation is flushed with dynamic coating solution after flushing with 1M NaOH and DI water before reusing it. The dynamic coating procedure is

very simple and quick to apply. Dynamic coating requires occasional regeneration, in addition to flushing the capillary with the coating solution. The coating material solution can also be added into the run buffer for regeneration of coating consistently throughout all runs. The dynamic coating is non-covalently bonded with a surface charge. The coating molecules physically adhere to the surface forming a layer. By the formation of adsorptive layer, dynamic equilibrium set up between the coating material adsorbed on the surface and the material flowing with the sample solution in the capillary.<sup>58</sup> This dynamic equilibrium between the adsorptive layer and run buffer has been illustrated in Fig 1.17 below.

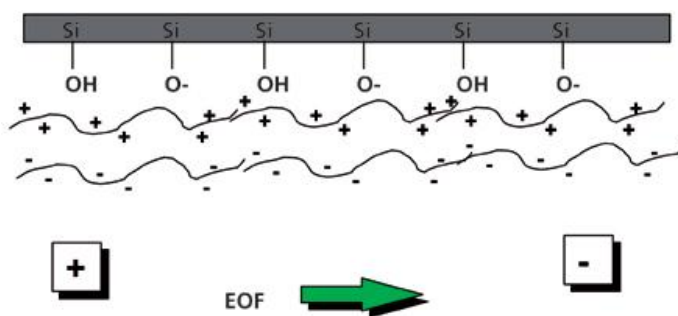


**Fig 1.17: Illustration of layers formation in dynamic coating.**<sup>64</sup>

There will be constant concentration of ions of electrolyte on both solution and the adhered layer because of dynamic equilibrium between the added layer and the run buffer. The coating molecules are absorbed on the capillary surface by weak interaction such as electrostatic attraction, van der Waals force, and hydrogen bonding. An illustration of dynamic coating and the EOF is shown in Fig 1.17. Layer by layer (LBL) self-assembly technique has been demonstrated by Haselberg et al which consists of triple layer polybrene - dextran sulfate-polybrene triple layer coating.<sup>61, 65</sup> In this project, EoTrol LN® copolymer has been used for a material for dynamic coating. It is a commercial name for a generic product N – substituted acrylamide copolymer.<sup>5</sup> It is a premade solution with a simple dilution with run buffer.

### ***1.8.2 Covalent coating***

A permanent capillary wall coating is an attractive way to eliminate EOF and wall-analyte interaction in the CE separations.<sup>60</sup> It is also known as covalent or static coating. Preparation of a permanent wall coating typically consists of three steps: capillary pretreatment, introduction of a double bond to the capillary wall and bonding of a polymer to the intermediate layer. To achieve the best coating result, the capillary surface must be cleaned and activated by etching (rinsing by NaOH), leaching (rinsing by HCl), dehydrated overnight at 160°C, silylation reaction before the coating process. The coating process involves attaching a polymer coating to the capillary wall using a reactive bifunctional silane such as  $\gamma$ -methacryloxypropyltrimethoxysilane as described by Hjarten et al.<sup>66</sup> The surface silanol then reacts with the silane group of the reagent; the other functional group is used to attach and polymerize monomers to the capillary surface. In another method, polymethacryloxypropylhydroxylsilane is used as an intermediate layer to form a resin in the deactivation reaction, which effectively covers any uncovered silanol groups.<sup>66</sup>

Malik and coworkers shortened several steps of covalent bonding in one step. First, capillaries were filled with a methylene polymer instead of a monomer such as HPC and PEI; a brief heat treatment was then used to immobilize the polymer film on the capillary surface.<sup>67</sup> In order to improve the stability of the coating at alkaline pH, Cobb and coworkers replaced Si-O-Si bonds with Si-C bonds using Grignard reagent chemistry. It was found that Si-C bond-based coating was stable up to 30 days at pH 2.3 to 9 at 30°C, while siloxane bonds are damaged at pH > 4.6. This method was later modified into large-scale production of permanently coated capillary arrays for DNA sequencing.<sup>68</sup>

In covalent coating, the surface of the capillary is transformed permanently by forming bond with uncapped silanol terminals and coating reagents. The EOF can be controlled or reversed by changing the surface charge.<sup>63</sup> Adsorption of proteins, particularly basic proteins onto fused silica capillaries severely degrades the capillary electrophoresis performance. Despite having advantages of high efficiency, high sensitivity, high speed and low effective, CE suffers a severe loss of resolution due to peak tailing.

## **1.9 Viruses**

Viruses are present in large numbers everywhere in nature, in the air, water and soil. We breathe viruses through air and eat viruses through various food materials and water. We easily come in contact with viruses like Influenza by touching door knobs, computer keyboards and stairs banisters. It is almost impossible to avoid coming in contact with viruses. Millions of people get sick from the flu, polio, and HIV every year. Virally caused human diseases include the flu, the common cold, herpes, measles, chicken pox, small pox and encephalitis. Viral diseases in humans are controlled by preventing transmission, taking vaccines and taking antiviral drugs. Similarly, millions of animals die due to viral infections every year. Swine flu and bird flu virus pandemic attacked several countries like China and South Asian countries during the last decade.<sup>69</sup> There are more species of viruses than any other living animal or plant on the earth. All species of plants and animals have their viruses. The word “virus” comes from the Latin word “virus” which refers to poison or other noxious substances. Louis Pasteur first speculated that there are pathogens that cause rabies and are too small to be detected by the light microscope. All viruses are not harmful as we normally think. For example, bacteriophage



viruses kill bacteria but are harmless to many other animals. There are over  $10^{30}$  different types of bacteriophage virus particles in water on the earth. A virus particle weighs about a femtogram ( $10^{-15}$ g). Most of the viruses which infect us have no impact on our health or wellbeing because our immune systems defend us from these viruses. Imaging of viruses became possible only after the invention of the electron microscope. Electron micrographs show that viruses exist in different shapes and sizes. A few examples are shown in Fig1.18. On the left is the bacteriophage virus T1, labeled as A. Bacteriophage virus capsid is called head and is polygonal in shape. It has a neck and tail consisting of protein and carbohydrate fibers. Similarly, Tobacco Mosaic Virus is rod - like in shape.<sup>70</sup> The rabies virus is in a capsule shaped,<sup>71</sup> and Rota viruses look like spheres with spikes

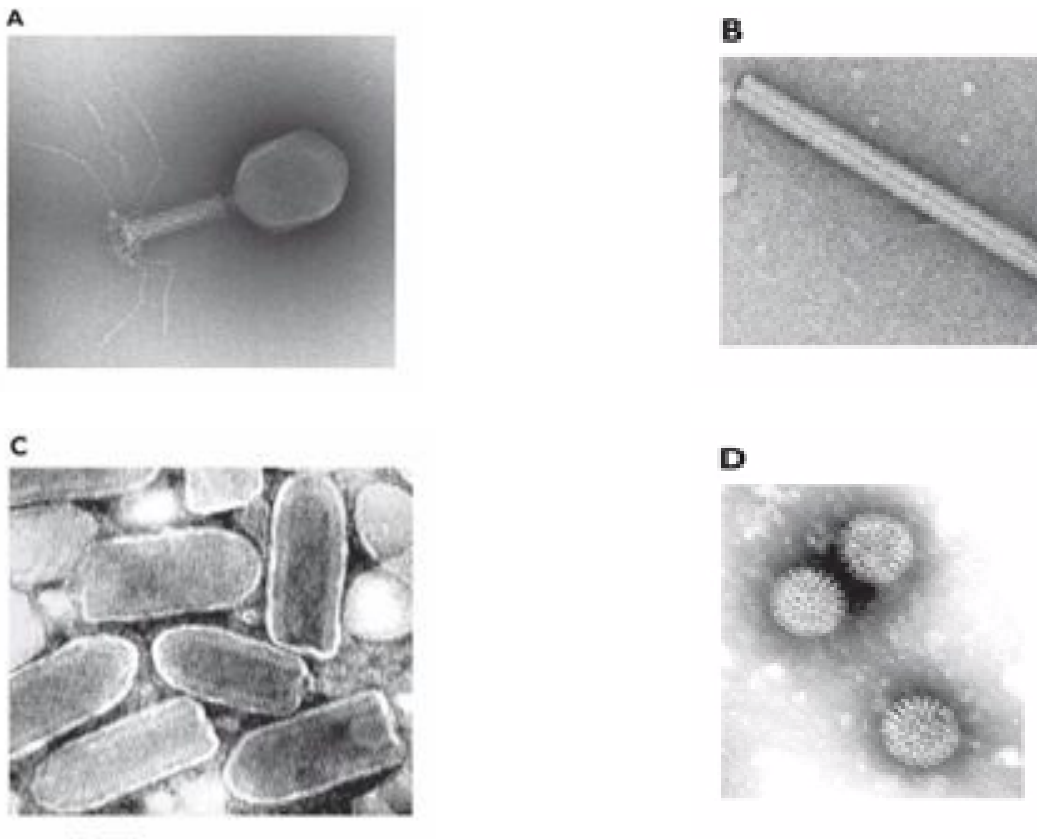


**Fig 1.18: Electron micrograph of bacteriophage T1 virus has polygonal head, neck and tail in Fig labeled A, Tobacco Mosaic virus in B is rod shaped and Rabi's virus has tablet**

**shaped in C and Rota virus is sphere shaped like solid sphere with a lots of spikes on its surface**<sup>72,73</sup>

A strange property of any viruses is that it can demonstrate characteristics of a lifeless particle in absence of host living cells, but it can replicate as soon as it gets into the living host cells.

### ***1.9.1 Structure of viruses***

All virus particles contain structure containing viral genome packaged in a protein coated called the capsid. For some viruses capsid is surrounded by lipid bilayer that contains viral proteins, usually including the proteins that enable the virus to bind to the host cells.

Bacteriophage viruses consist of a head, neck, and tail.<sup>74</sup> The head, which is also called the capsid, encloses specific type of genomes either DNA or RNA by specific type of proteins and lipid layer (also called envelope). The capsid and envelope play many roles in viral infection, including virus attachment to cells, entry into cells, release of the capsid contents into the cells, and packaging of newly formed viral particles. The capsid and envelope are also responsible for transfer of the viral genetic material from one cell to another.

There are mainly seven different types of viral genome, mainly consisting of single and double stranded DNA and RNA including mixed and positive and negative RNA.<sup>74</sup> The double stranded structure of DNA (Deoxyribonucleic Acid) consists of thousands of nucleotides (phosphate , deoxyribose sugar and one of nucleic acid bases - adenine, thymine, guanine and cytosine) polymerized and bind together by hydrogen bonds between base pairs of single strands. But RNA (ribonucleic acid) is single strand that consists of a phosphate, ribose sugar and one of the nucleic acid bases - thymine, uracil, guanine and cytosine. The genome types differ in their protein composition and gene sequences.

In addition to genome type, shape and size of viruses are important for viral detection and identification. Viruses occur in various shapes and sizes from a few nanometers to a few hundred nanometers long but all contain a capsid but not all contain envelop. The capsid and envelop structures also determine the stability characteristics of the virus particles such as resistance to the chemical and physical inactivation. For identification of viruses, the proteins finger different viruses are obtained by various spectroscopic and analytical techniques like Raman spectroscopy, laser-induced fluorescence and UV absorption spectroscopy coupled with isoelectric focusing (IEF).

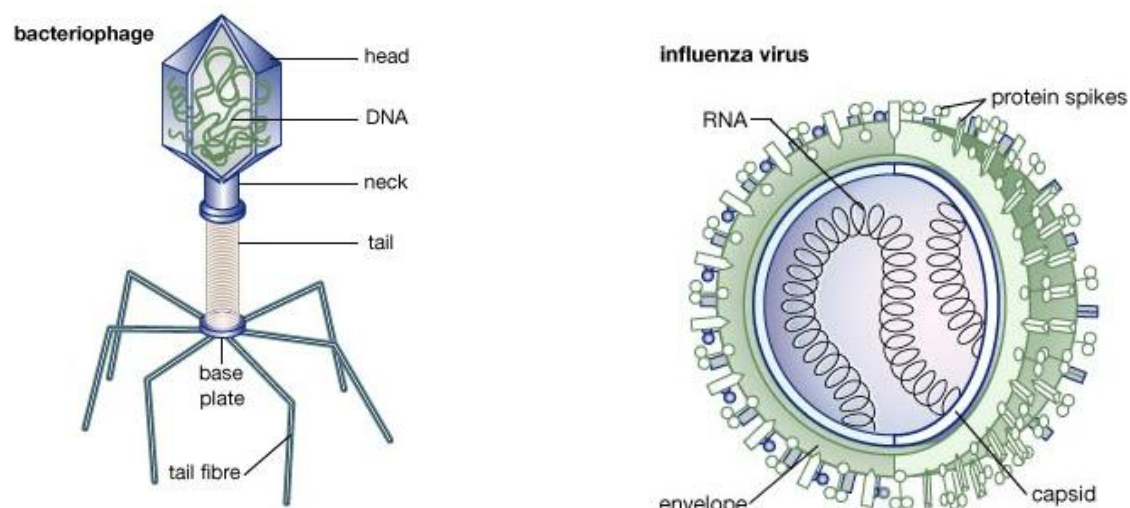


**Fig 1.19: Schematics of structure of viruses.** <sup>71</sup>

Besides spectroscopic method, performing IEF in a gel can be performed but requires a tedious protocol for sample preparations, and long data analysis time, usually three to four hours if not days. The electron microscope is the ultimate instrument for virus imaging<sup>75</sup> but is very expensive, requires extensive sample preparation and lacks portability. Capillary isoelectric focusing (cIEF) is one of the very simple, robust and efficient techniques which can be employed for rapid detection and separation of live microorganisms like viruses,<sup>76</sup> bacteria<sup>77</sup> and other single

cells.<sup>78,79</sup> Application of cIEF for separation and detection viruses is considered feasible because they contain specific proteins and net surface charge due to terminal amino or carboxylic acid groups. Depending on the environment pH, protonation or deprotonation on these terminal groups lead to a certain value of overall charge in the protein. The main sources of charges on the living cell are the amino acids and the way they are sequenced in the proteins and peptides. Since virus particles have overall charge at specific pH so they are separable and detectable by cIEF. This technique has a potential for application to on-site detection of all other parasites as well.<sup>80</sup> In this project, isoelectric focusing techniques have been used to detect and identify viruses based on their isoelectric point, though impurities and contaminants might lead to some confusion. The focused bands of viruses were detected by a UV light absorbance measurement at 280 nm.<sup>81</sup>

## Chapter 2 - Experimental Procedures

### 2.1 Materials and Methods

Sodium Borate was obtained from Fisher Scientific. RhodamineB and Rhodamine6G<sup>+</sup> were obtained from Acros organic. cIEF Anolyte (100mM phosphoric acid), Catholyte (100mM NaOH) and Servalyte® were obtained from Bio-Rad (Hercules, CA). EuTrol LN® was purchased from Target Discovery. Standard proteins, namely, liposome, cytochrome C, myoglobin (equine), insulin (human), bovine serum albumin (BSA) lyophilized powder Biotech Grade were obtained from Fisher BioReagents. Bacteriophage viruses T1 and TR4 were obtained from obtained from Prof Jun Li's labs which were cultured in E.coli bacteria as host cells. The following five different standard proteins solution were prepared; Bovine serum albumin (BSA) (0.1% w/v), cytochrome C (0.1% w/v), lysozyme (egg white) (0.1%) and myoglobin (equine) (0.1 % w/v) in 2% Servalyte® (pH 3-10). 5% EoTrol LN® solution for coating was made separately in 30 mM/L Tris HCl buffer. UV spectrometer was set at a wavelength at 280 nm, absorbance 0.03, and sensitivity 0.02. After conditioning the capillary according to manufacturer's protocol, 1:19 EoTrol LN® and Servalyte mixtures were passed through the capillary for 2 minutes with the help of a syringe pump. Then in order to load a sample into the capillary for focusing, EoTrol LN®, Servalyte® and the protein of interest were mixed and then passed through the capillary with the help of syringe pump. After the loading step, one end of the capillary was inserted into a reservoir containing Bio-Rad Catholyte (100mM NaOH) and the other one was inserted into Bio-Rad Anolyte (100 mM H<sub>3</sub>PO<sub>4</sub>). Afterward the anode from higher power supply was introduced into the reservoir containing anolyte and the cathode was inserted

into the catholyte reservoir. Then the electric potential was applied. The current increased very rapidly to a peak value of 25  $\mu\text{A}$  to 30  $\mu\text{A}$  and then gradually decreased to a much lower stable current (4  $\mu\text{A}$ ). If no current or a rapid fluctuation of current was observed, that indicated either the capillary was clogged or an air bubbles was trapped inside of the capillary. In such a case, the experiment was repeated from preconditioning step to focusing. A stable low current after a few minutes indicated the completion of focusing. Now, in order to mobilize focused band of protein to the detector, the anolyte  $\text{H}_3\text{PO}_4$  was changed with tube containing 66% NaCl and 33% NaOH solution. Again the voltage was resumed; the current increased again indicating the movement of ions in the capillary. In the computer screen, the intensity versus mobilization time data acquired by LabVIEW program was saved for further analysis. After completion of cIEF of five proteins, T4R virus and T1 virus was loaded in a separate run for cIEF and the absorption peak (intensity vs mobilization time) obtained then this data was saved for analysis.

## 2.2 Solution Preparation

A pH 9.1 25 mM sodium borate buffer was made by dissolving 2.41 g  $\text{Na}_2\text{B}_4\text{O}_7$  in 250 mL of 18M $\Omega$  water and mixed with 4.7 mL of 0.1 M HCl. The 1mM Rhodamine B and Rhodamine6G<sup>+</sup> solution was made in 20 mL of DI water. A 1M NaOH solution was made by dissolving 4.0 g of NaOH in 100 mL of DI water. 0.1 mM and 0.001 mM NaOH solutions were made by diluting the concentrated solution appropriately. 20 mL of a 1 mM NaCl solution was made by dissolving 11.7 g sodium chloride into DI water. The EoTrol LN<sup>®</sup> solution for the dynamic coating was prepared according to the protocol provided in the purchased sample. In this protocol 1 part of EoTrol LN<sup>®</sup> was dissolved with 19 parts of run buffer so 0.5 mL of EoTrol LN<sup>®</sup> was mixed with 9.5 mL of buffer pH 9.1. For silane-based reagent coating, a 2%

silane solution was prepared by dissolving 500  $\mu\text{L}$  of 3 – methoxyacryloxypropyl trimethylethoxysilane in 95% EtOH to make 25 mL of stock solution 30 mM Tris HCL pH 9.1 was used as run buffer for cIEF of proteins. To make 10mL of 0.1% w/v concentrated solutions of each of five proteins, BSA, cytochrome C, lysozyme (egg white) and myoglobin (equine), calculated amount of proteins were dissolved in run buffer for cIEF experiment.

### **2.3 Capillary cutting, preconditioning**

First two capillaries were prepared cIEF experiment from bundle of capillaries of beginning ID 52.1  $\mu\text{m}$ . Capillary labeled ‘1’ was 49.3 cm long and the effective length measured from the window to the longer end is 42.6 cm. Capillary ‘2’ was 48.7 cm long and the effective length measured was 40.0 cm. A window was burned carefully to make as narrow as possible by exposing a small region of capillary to a flame. Then the burned portion of the capillary was wiped with chemwip gently soaked with methanol which removes the outer coating of the fused silica capillary. The effective length of capillary was measured from the longer side from the detection window. The capillary window was carefully aligned with the detection optics on the UV/VIS detector and secured with screws and cover. The capillary was first flushed with 1 M NaOH using a syringe and filter pump for 5 minutes at rate of 90  $\mu\text{L}/\text{min}$ . Then it was flushed with 0.1 mM NaOH and sodium borate buffer for 5 minutes each with the same rate. This step ionizes and activates the capillary surface for CE. The capillary was flushed with methanol for 10 minutes with the help of syringe pump at rate of 90  $\mu\text{L}/\text{min}$ . DI water was pumped through the capillary at the rate of 90  $\mu\text{L}/\text{min}$  for 4 minutes. After that 1M HCl was flushed for 10 minutes at the same rate. Again, DI water was flushed through the capillary for 4 minutes.

## **2.4 Dynamic coating procedure**

After flushing the preconditioned capillary with the reagents in series as following 1M NaOH for 5 minutes, 0.1 M NaOH for 2 minutes, 0.1 M HCl for 5 minutes and DI water for 5 minutes, 5% EoTrol LN® coatings was flushed through the capillary for 5 minutes. Then mixture containing 5% EoTrol LN®, 4% Servalyte ® (pH 3 to 10) and 0.1% marker protein was passed into the capillary for 2 minutes with the help of syringe pump. Then electrodes, cathode in catholyte and anode in anolyte contained in the reservoir were inserted. Then 20 kV electric potential was applied through the electrodes across the capillary. The current increased to around 30 to 40  $\mu$ A during the focusing at the beginning but gradually decreased to 6 to 10  $\mu$ A after 5 to 10 minutes. This stable lower current was an indication of completion of focusing. For online single point detection, anolyte vile was replaced with a tube containing neutral salt solution and high voltage supply of 20 kV was resumed. After reapplying electric field, the current started increasing rapidly but after around 10 minutes current levels off. This procedure for moving focused bands past the detector is called mobilization. During mobilization coating reagents were not added. Once mobilization was complete for the run, again capillary preconditioning procedure was repeated to provide coating on the wall before injecting sample mixture for another run. Before injecting the protein for focusing, repeated preconditioning and fresh coating was performed to improve reproducibility of run and eliminate the effect of previous runs.

## **2.5 Capillary Electrophoresis: injection mode and run time**

Eppendorf® tubes were used as buffer reservoirs and situated at the same height so that so siphoning occurred. A third Eppendorf® tube containing the mixture of Rhodamine B and Rhodamine6G<sup>+</sup> in buffer was used as a sample container. The anode and cathode from high



power supply were inserted into the buffer reservoirs. The capillary was equilibrated by applying 5 kV across the capillary until the current stabilized. To make an injection, the anode end of the capillary was inserted into the sample solution containing RhB and Rh6G<sup>+</sup> kept in tube 3 for CE. A 20 seconds long injection at 5 kV was made, the capillary was returned to the run buffer and 20 kV electric potential was applied for 2000s. This process was repeated until reproducible result is obtained. This procedure was performed for each capillary. The migration times are recorded for each of CE run for the mixture of RhB and Rh6G<sup>+</sup>.

## 2.6 EOF determination

In this experiment, different alkoxy alkyl silane-based coating reagents were tried but only data from coatings made with 3-methacryloxypropyl trimethoxysilane and a commercial available reagent trade name EoTrol LN® polymer LN (N-substituted acrylamide co-polymer solution, 0.1 to 1.5 % acrylamide) from Target Discovery are reported. The other two silane based reagents - cyclohexyltrimethoxysilane and 3 - iodopropyl trimethoxysilane were found not to reduce the EOF significantly. For the EOF determinations, 1mM RhB solution was injected for 20 s at 5 kV. The EOF was determined from the migration time of a neutral EOF marker dye (i.e. Rhodamine B) in the CE experiment. From the migration time of RhB, the velocity was calculated by dividing effective length of capillary to obtain the electroosmotic velocity. Once electroosmotic velocity was calculated, it is divided by electric field strength to determine the electroosmotic mobility. Effective coating materials will eliminate most of the EOF and make it difficult to determine an exact EOF value. However, if the electrophoretic mobility (EP) of a charged compound is already determined then the EOF can also be determined. For an example, the EOF and EP mobility of a charged compound was determined with a mixture of RhB and

Rh6G<sup>+</sup> in an uncoated capillary as below. The migration times of RhB and Rh6G<sup>+</sup> can be used to calculate electrophoretic mobility ( $\mu_{ep}$ ) for R6G<sup>+</sup>.

For RhB, electroosmotic velocity in uncoated capillary is calculated, dividing effective length of capillary by migration time of RhB as it is neutral molecule  $v_{eo} = 42.6 \text{ cm} / 298 \text{ s} = 0.142 \text{ cm/s}$ . Electroosmotic mobility of the molecule is then calculated by dividing electroosmotic velocity by field strength as  $\mu_{eo} = v_{eo} / E = (0.143 \pm 0.004) \text{ cm/s} / (20000 \text{ V} / 49.3 \text{ cm}) = 3.57 (\pm 0.01) \times 10^{-4} \text{ cm}^2/\text{Vs}$ . Similarly, for Rh6G<sup>+</sup> molecule, total electrokinetic velocity and mobility are calculated as  $v_{ek} = (42.6 \pm 0.10) \text{ cm} / (181 \pm 8) \text{ s} = 0.235 \pm 0.001 \text{ cm/sec}$  and  $\mu_{ek} = 0.235 \pm 0.001 \text{ cm/s} / (2.0 \times 10^3 \text{ V} / 49.3 \pm 0.10 \text{ cm}) = 5.8750 (\pm 0.0006) \times 10^{-4} \text{ cm}^2/\text{V}$  respectively. Since EOF is already determined using RhB, electrophoretic mobility is obtained subtracting electroosmotic mobility from electrokinetic mobility.  $\mu_{ep} = 5.8750 (\pm 0.0006) \times 10^{-4} - 3.57 (\pm 0.01) \times 10^{-4} = 2.30 (\pm 0.01) \times 10^{-4} \text{ cm}^2/\text{Vs}$ . If the capillary was then coated, the migration time of R6G<sup>+</sup> can be used to determine the EOF because  $\mu_{ep}$  has already been determined. For the example in silane based reagent coating  $v_{ek} = (40 \pm 0.1) \text{ cm} / (399 \pm 3) \text{ s} = 0.100 (\pm 0.0003) \text{ cm/s}$ . Electrokinetic mobility of Rh6G<sup>+</sup> in the capillary with silane-based coating is calculated as  $\mu_{ek} = v_{ek} / E = 0.1002 (\text{cm/s}) / (20,000 \text{ V} / 48.7 \text{ cm}) = 2.4634 (\pm 0.0002) \times 10^{-4} \text{ cm}^2/\text{s}$ . Now, residual EOF of coated capillary can be determined by migration time of RhB dye which is  $1.5 (\pm 0.02) \times 10^{-4}$ . Therefore, the percentage reduction of EOF compared with uncoated capillary is  $58.0 \pm 3\%$  as calculated below.

$$\% \text{ EOF reduction} = (3.57 (\pm 0.01) \times 10^{-4} - 1.5 (\pm 0.02) \times 10^{-4}) / 1.5 \times 10^{-4} = 58.0 \pm 3$$

Similarly, for a capillary with EoTrol LN® coatings, EOF cannot be determined using RhB dye because EOF was reduced significantly so second peak for RhB didn't appear in the electropherogram within 2000 s long run of buffer. Therefore EOF was calculated by subtracting

electrophoretic mobility of Rh6G<sup>+</sup> which has been already determined from electrokinetic mobility of Rh6G<sup>+</sup>. Since electrophoretic mobility also depends inversely with the viscosity of the electrolyte, any change in the composition of electrolyte would result different electrophoretic mobility of the same Rh6G<sup>+</sup>. This can be seen in table above that electrophoretic mobility of Rh6G<sup>+</sup> changes with the change in the coating material. For regeneration of coatings, solution of coating material was added in the sample solution and also in the run buffer; viscosity of buffer in bare, silane-based reagent and EoTrol LN® coating was slightly different due to the different nature of coating material.

Electropherograms of RhB and Rh6G<sup>+</sup> indicating migration times were collected by data acquisition program of LabVIEW and were analyzed using Igor Pro data analysis software. The data of electropherogram was loaded into binary delimited file format and the wave was scaled to account for the 10 Hz data acquisition rate (DAR). The data were smoothed by factor of 50 using a binomial smoothing algorithm. The sensitivity (Absorbance units/V) was set at 0.01 or 0.005 depending on the analyte used. The wave length was set at 465 nm. The run buffer used for CE of RhB and Rh6G<sup>+</sup> CE mixture was 50:50 with 10 mM methanol and 10 mM sodium borate buffer. The silane based reagent was also added with the sample mixture of 0.3 mM RhB and 0.3 mM Rh6G<sup>+</sup> for coatings of capillary walls. For EoTrol LN® coatings and 5µL of 5% EoTol LN® mixed with the 5mL of fluorescent dye mixture with 5 mL run buffer. Injections were made for 20 s at 5 kV. The run time and run voltage were set at 2000 seconds and 20 kV.

### ***2.6.1 Experimental Setup***

Experiment set up cIEF experiment was exactly same as CE as shown in Fig 2.1. The only difference was, the cathode and anode buffer reservoirs of CE were replaced by 0.02 M

NaOH catholyte and 0.02 M  $\text{H}_3\text{PO}_4$  analyte. The wavelength of light was changed to the UV region because the most proteins absorb in the UV region at around 280 nm to 320 nm. For loading the proteins and Servalyte® solution, a syringe with a micro filter and a syringe pump was used. The mixture was loaded in the capillary for 2 to 3 minutes. After loading the sample, electric field was applied through the platinum electrodes inserted into the reservoirs.

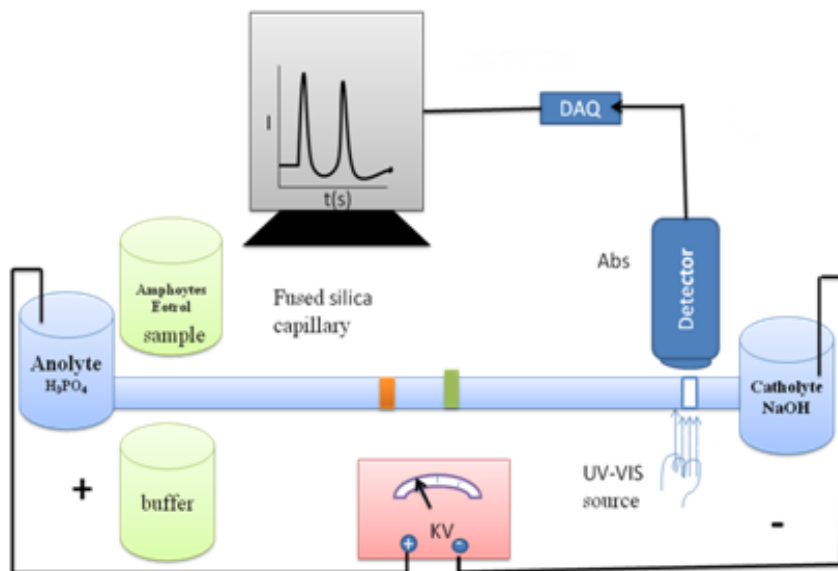


**Fig 2.1: Experimental set up for cIEF.**

### 2.6.2 Detection

Detection of RhB and Rh6G<sup>+</sup> dyes flowing through the capillary was performed by on column single point detection method. For this purpose, a narrow window was burned on the capillary near the cathode. Then it was aligned very carefully and held fixed on the optics of detector. In order to make sure that there was not stray light entering through detection point, a black lid was attached on the detector window and screwed properly. This also prevents capillary slipping away from the detection point in detector. On column single point detection mode was used for the all measurements in the experiments presented in this thesis.

### ***2.6.3 Isoelectric focusing of proteins***

Five proteins pI, which were determined by other methods and reported in different journals are given in this thesis: cytochrome C (pI =11.4), lysozyme (egg white) (pI =9.2), myoglobin (equine) (pI =7), and human insulin (pI = 5.3). The pIs reported were also slight different values if the sources of these proteins were different. After setting experimental parameters as mentioned already in the experimental and procedure section, isoelectric focusing was carried out using Servalyte® as an ampholytes and EoTrol LN® polymer LN for coating material to suppress the effect of the EOF during separation process and to reduce protein adsorption on the surface. Sample tube containing EoTrol LN®, ampholytes and buffer was filled into the capillary with the help of syringe and pump without trapping air inside the capillary. After loading the capillary with sample proteins and ampholytes, 20 kV DC was applied across the capillary via anode and cathode whose ends were attached with a platinum wire for the portions which were immersed into catholyte and anolyte vials. The platinum metal is inert metal so it doesn't react with any reagents. If electrode with platinum were not used, it would react with acid in anolyte and produces gas in the mixture. If air or gas bubble trapped in the capillary it interrupts current flow during focusing and ruin the experiment completely. Therefore it is extremely important to used degassed buffer and inert electrodes in all CE and cIEF experiment.

#### ***2.6.4 Mobilization procedure of proteins***

In order to detect the focused bands of the proteins separated by cIEF, the bands were driven past the UV detector for on column single point detection. The bands were mobilized by anodic mobilization, in which anolyte was replaced by a solution consisting 0.02 M acetic acid and 0.04 M NaCl. During mobilization, 20 kV electric field was applied through the electrodes. As the mobilization starts, the current gradually increases from the low current until to certain high until voltage was applied. Adding non proton cations ( $\text{Na}^+$  and  $\text{CH}_3\text{COO}^-$ ) containing solutions in anolyte shifts the pH in the capillary progressively then the proteins acquire charge again and proteins moved towards the detector under the influence of electric field.

## Chapter 3 - Coatings efficiency via EOF determination

The coating efficiency on a fused- silica capillary was evaluated by measuring the EOF of two dyes RhB and RhG<sup>+</sup>. The reasons for choosing these two dyes were 1) both have strong absorption in the visible region,  $\lambda_{\max} = 553 \text{ nm}$  for RhB and  $\lambda_{\max} = 524 \text{ nm}$  for Rh6G<sup>+</sup>, and 2) RhB being a neutral molecule can be used to determine the EOF and Rh6G<sup>+</sup> being positively charged will migrate to the cathode, even without the EOF. The data obtained from the CE experiments with two dyes, RhB and Rh6G<sup>+</sup> in a capillary without coatings (bare capillary) and a capillary dynamically coated with silane-based reagent and EoTrol LN® are summarized in the table1.

### 3.1 CE of RhB and Rh6G<sup>+</sup> without and with silane-based reagent coating

From the migration time of RhB,  $298 \pm 8 \text{ s}$  with RSD 2.7% from the graph in Fig 3.1, electro-osmotic mobility was calculated as  $3.57 (\pm 0.01) \times 10^{-4} \text{ cm}^2/\text{Vs}$  in a bare capillary. From the migration time of Rh6G<sup>+</sup>  $181 \pm 1 \text{ s}$  with RSD 0.5%, the electrokinetic mobility was calculated to be  $5.8750 (\pm 0.0006) \times 10^{-4} \text{ cm}^2/\text{Vs}$ . Rh6G<sup>+</sup> being a positively charged molecule experiences combined effect of the EOF and the electric field applied in its migration. Therefore, the net electrophoretic mobility of positively charged dye molecules is calculated by the difference in electrokinetic and electroosmotic mobility. Hence the electrophoretic mobility of Rh6G<sup>+</sup> is calculated as  $2.30 (\pm 0.01) \times 10^{-4} \text{ cm}^2/\text{Vs}$  with RSD < 1%. Then the capillary was coated with a silane based reagent, 3-methylacryloxypropyltrimethoxysilane (MAPTMS) (C<sub>10</sub>H<sub>22</sub>O<sub>4</sub>Si, Mol. Wt 234.36 Da). Different migration times for the neutral dye RhB of  $651 \pm 8 \text{ s}$  with RSD 1.3% and charged dye molecule Rh6G<sup>+</sup> of  $399 \pm 3 \text{ s}$  in a mixture injected together were obtained.

**Table 1: Summary of migration times and mobilities.**

Capillary	Uncoated (42.6 ± 0.1 cm)		Silane-based reagent (40 ± 0.1 cm)		EoTrol LN® coated (42.6 ± 0.1 cm)	
molecule	RhB	Rh6G <sup>+</sup>	RhB	Rh6G <sup>+</sup>	RhB	Rh6G <sup>+</sup>
t <sub>mig</sub> (s)	298 ± 8	181 ± 1	651 ± 8	399 ± 3	NA	819 ± 20
%RSD	2.8	0.5	1.3	0.8		2.4
v <sub>eo</sub> /v <sub>ek</sub> (cm/s)	0.143 ± 0.004	0.235 ± 0.001	0.614 ± 0.007	0.1002 ± 0.0003		0.052 ± 0.001
μ <sub>ek</sub> (cm <sup>2</sup> /Vs)		5.8750 (± 0.0006) x10 <sup>-4</sup>		2.4634 (±0.0002) x10 <sup>-5</sup>		1.27 (±0.03) x10 <sup>-4</sup>
μ <sub>eo</sub> (cm <sup>2</sup> /Vs)	3.57 (± 0.01) x10 <sup>-5</sup>		1.5 (± 0.02) x10 <sup>-4</sup>		3.5 (± 0.06) x10 <sup>-5</sup>	
μ <sub>ep</sub> (cm <sup>2</sup> /Vs)		5.52 (± 0.01) x10 <sup>-4</sup>		9.5 (± 1.9) x10 <sup>-5</sup>		9.5 (± 0.5) x10 <sup>-5</sup>
EOF (%) reduction			58 (± 3)		90 (± 3)	

**Table 2: Summary of migration times, % RSD, quality of separation (N), and Resolution (Rs)**

Capillary	Uncoated		Silane – based reagent coated		EoTrol LN® coated	
molecule	RhB	Rh6G <sup>+</sup>	RhB	Rh6G <sup>+</sup>	RhB	Rh6G <sup>+</sup>
t <sub>mig</sub> (s)	298 ± 8	181 ± 1	651 ± 9	399 ± 3		819 ± 20
%RSD	2.7	0.57	1.3	0.8		2.4
(ω <sub>1</sub> /ω <sub>2</sub> ) <sub>av.</sub>	5 ± 1	3.3 ± 0.5	7 ± 1	9 ± 2		12 ± 2
N	24,000 ± 5,000	17,000 ± 4,000	43,000 ± 8,000	26,000 ± 15,000		26,000 ± 7,000
Rs	17 ± 6		22 ± 4		Only one peak	



The electroosmotic velocity for RhB is 0.143 cm/s with error  $\pm 4.0 \times 10^{-3}$  due to standard deviation  $\pm 8$  s in migration times. In the same way, electroosmotic velocity for RhG<sup>+</sup> was calculated as  $0.235 (\pm 0.01) \times 10^{-3}$  cm/s. For both of these runs, the effective length of capillary was 42.6 cm and preconditioned with 1 M NaOH, 0.1M NaOH followed by 0.1 HCl. Then finally the capillary was washed by double distilled water. The electroosmotic and electrokinetic mobility for RhB and Rh6G<sup>+</sup> were calculated to be  $3.57 (0.01) \times 10^{-4}$  cm<sup>2</sup>/Vs and  $5.8780 (\pm 0.0006) \times 10^{-4}$  cm<sup>2</sup>/Vs respectively. From the calculated result suggest that percentage reduction of the EOF with the silane-based coating is  $58 \pm 3$ . However, a dynamically coated lumen of a fused silica capillary with EoTrol LN® reduced the EOF by  $90 \pm 3\%$  compared to that of non-coated capillary.

The separation quality (N) of the peaks from CE of the two dyes RhB and Rh6G<sup>+</sup> in bare capillary was calculated to be  $24,000 \pm 5,000$  and  $17,000 \pm 4,000$  theoretical number of plates. But separation quality in the capillary after the silane-based reagent coatings capillary was increased to  $43,000 \pm 8,000$  and  $26,000 \pm 15,000$  for the same dyes Rhh6G<sup>+</sup> respectively. Resolution of peak was increased from  $17 \pm 6$  for uncoated capillary to  $22 \pm 4$  with silane based reagent coated capillary. There are some probably sources of errors which might have caused this variation in the migration time of analytes during CE such as injection plug length, detection, buffer concentration, pH of the solution, field strength due to the unequal capillary lengths, and distance of the detection window from electrodes might occur randomly. All above sources of errors independently contributed in the cause of variation of the migration time.

Above standard deviation in the migration time might have occurred mainly due to unequal time of silanization by flushing 1 mM NaOH and 0.1 mM NaOH prior to sample injection.

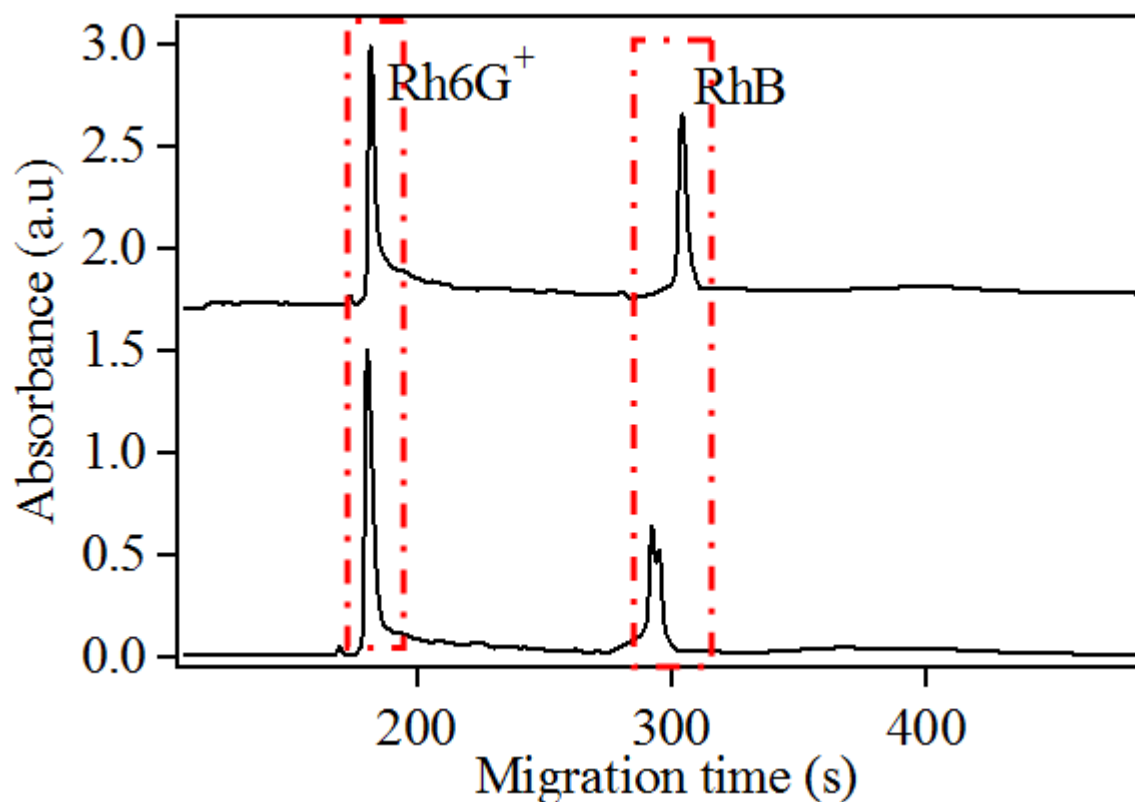


**Fig 3.1: Electropherogram of RhB and Rh6G<sup>+</sup> obtained by CE with preconditioned capillary without any coating. Migration times of Rh6G<sup>+</sup> and RhB 181 ± 1 s with 0.5 % RSD and 298 ± 8 s with 2.3 % RSD respectively.**

Time of silanization was not constant in all runs. Therefore, a little variation in the migration was expected. Unequal charge arising from unequal ionization of – SiOH groups on the capillary surface and magnitude of electric field applied makes significant difference in the consistency on the migration time and reproducibility in the electroosmotic mobility. Trapping air bubbles while flushing with NaOH and running a buffer was a common problem but it can be easily avoided using completely degassed buffer and careful insertion of capillary into the syringe and buffer vial.

### 3.2 CE of RhB and Rh6G<sup>+</sup> with EoTrol LN<sup>®</sup> coating

The CE with EoTrol LN<sup>®</sup> polymer coated capillary revealed only one peak within run time of 2000 s as in Fig 3.3. This provided a direct evidence of effectiveness of reduction of charge on the capillary surface by EoTrol LN<sup>®</sup> coating. RhB being a neutral analyte cannot flow as fast as Rh6G<sup>+</sup> does under the electric field. The migration times of Rh6G<sup>+</sup> in the capillary without and with coating were obtained as shown Fig 3.1 and Fig 3.2. Injection for first the run was made 10 s but second one was for 20 s which is obvious from the difference in the height of the peaks of in Fig 3.2. The summary table 1 shows that the dynamic coating with EoTrol LN<sup>®</sup> was more effective than silane based reagent coating as indicated by the percentage of electroosmotic

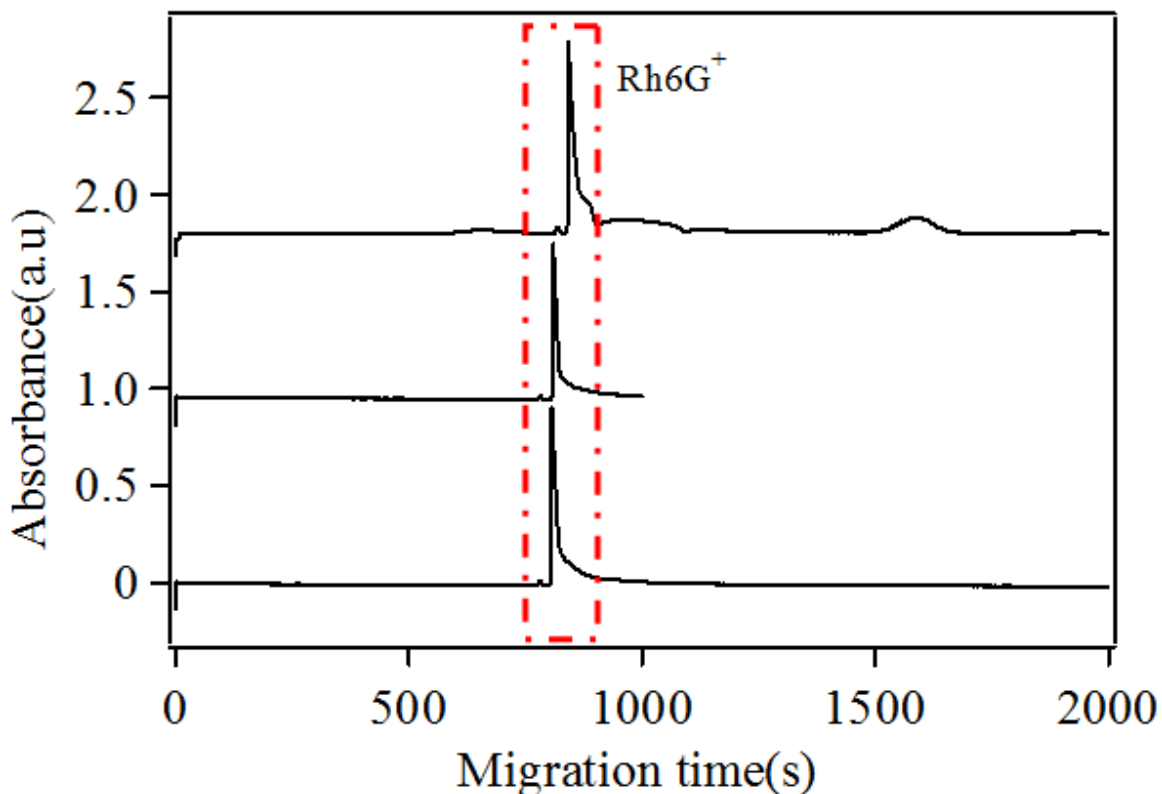


**Fig 3.2: Electropherogram RhB and Rh6G<sup>+</sup> mixture obtained by CE of with EoTrol LN<sup>®</sup> polymer coated capillary. The electropherograms of three consecutive runs with migration time  $819 \pm 20$  s with 2.4 % RSD.**

mobility reduction to  $90 \pm 3\%$  from the electroosmotic mobility of a bare capillary. Using the migration time of  $\text{Rh6G}^+$  with EoTrol LN<sup>®</sup> in the coated capillary, total electrokinetic mobility of positively charged molecule  $\text{Rh6G}^+$  was calculated to be  $1.27 (\pm 0.03) \times 10^{-4}$ .

The electropherogram with EoTrol LN<sup>®</sup> coating reveals the migration time of  $\text{Rh6G}^+$  is  $819 \pm 20$  s which is about 2.4% RSD due to the difference of migration times of different runs. One the most likely cause of this variation might be due to the difference of unequal height of sample and buffer reservoirs. This difference in height alters the length of injection due to collective contribution from both electrokinetic and hydrodynamic injection at the same time. The height adjustment was made just by long wooden ruler without proper level indicating devices. To find the reason why the second peak was not seen within 2000 s long run in the capillary as in Fig 3.2, the impact of coatings on capillary surface should be taken into the consideration. The separation quality (N) for  $\text{Rh6G}^+$  has marginally increased to 26,000 theoretical number plates compared to silane based reagent coatings. From all these calculation and observation, it becomes clear that EoTrol LN<sup>®</sup> copolymer was more effective for dynamic coating of capillary surface to suppress EOF.

### **3.3 cIEF of proteins and Viruses**

cIEF separations of myoglobin and lysozyme, BSA, Insulin, and cytochrome C followed by anodic mobilization were performed. Fig 3.3 and Fig 3.4 are representative electropherograms of five proteins. To order to avoid too many figures of all five proteins, separation data for BSA, Insulin, and cytochrome C are provided only in the summary table 3.3. The reported pI of all five proteins was plotted as a function of the mobilization time of protein in anodic mobilization.

**Table 3: Summary contains mobilization time of standard proteins, reported pI range, masses and number of amino acids and charge of the proteins in high and low pH.**

Proteins	Amino acids	Charge of protein at pH		Mass (kDa)	Mobilization time (s)	Reported pI
		Low	High			
Lysozyme	129	+	-	14.3	299 ± 22	11.0 -11.4
Cytochrome C	104	+	-	12	304 ± 23	9.1 - 10.1
Myoglobin	153	+	-	17.2	920 ± 31	6.8 - 7.2
Insulin	51	+	-2 to -6	5.3	1020 ±10	5.3 - 5.4
BSA	605	+21 ± 1.0	-17.0 ± 1	66.4	1072 ± 243	4.7 - 5.3

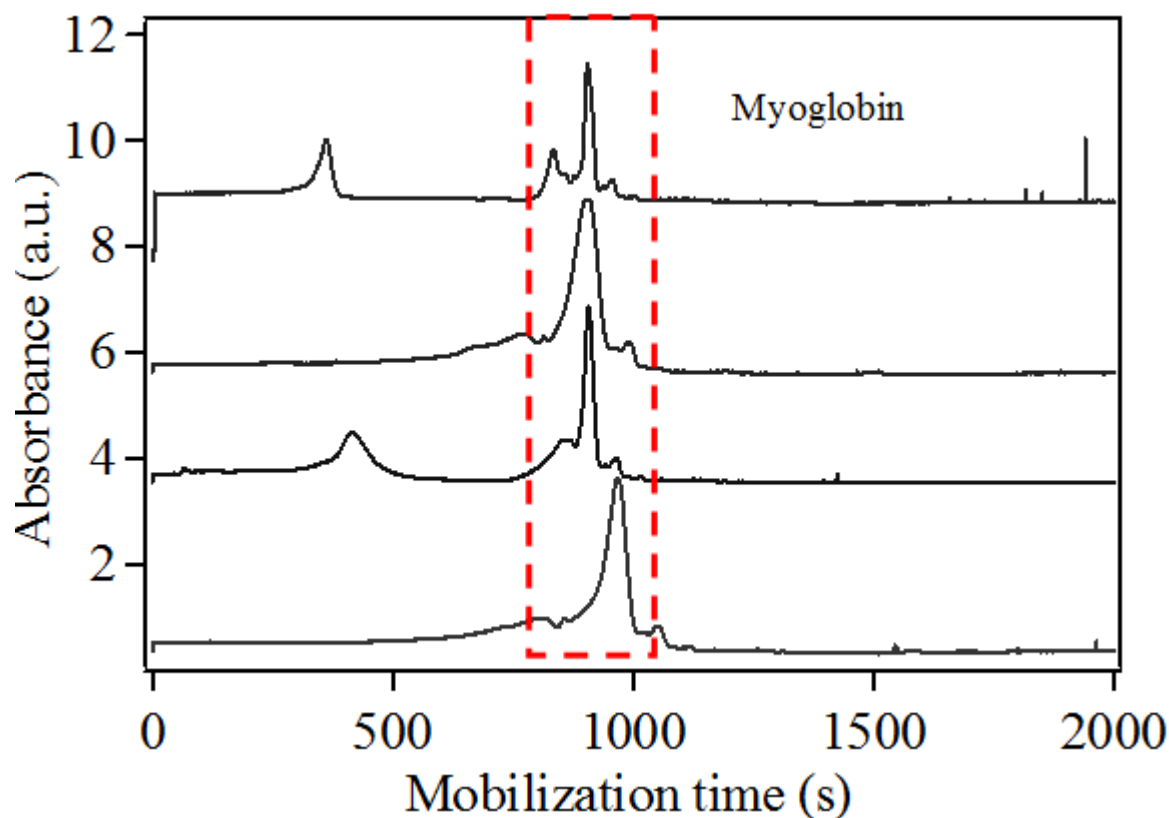


**Fig 3.3: Electropherogram of four consecutive runs of IEF of Myoglobin (equine) in an EoTrol LN® coated capillary followed by anodic mobilization with 66% NaCl and 33% NaOH mixture by volume. Mobilization time of Myoglobin is 920 ± 31 s with RSD of 3.4%.**

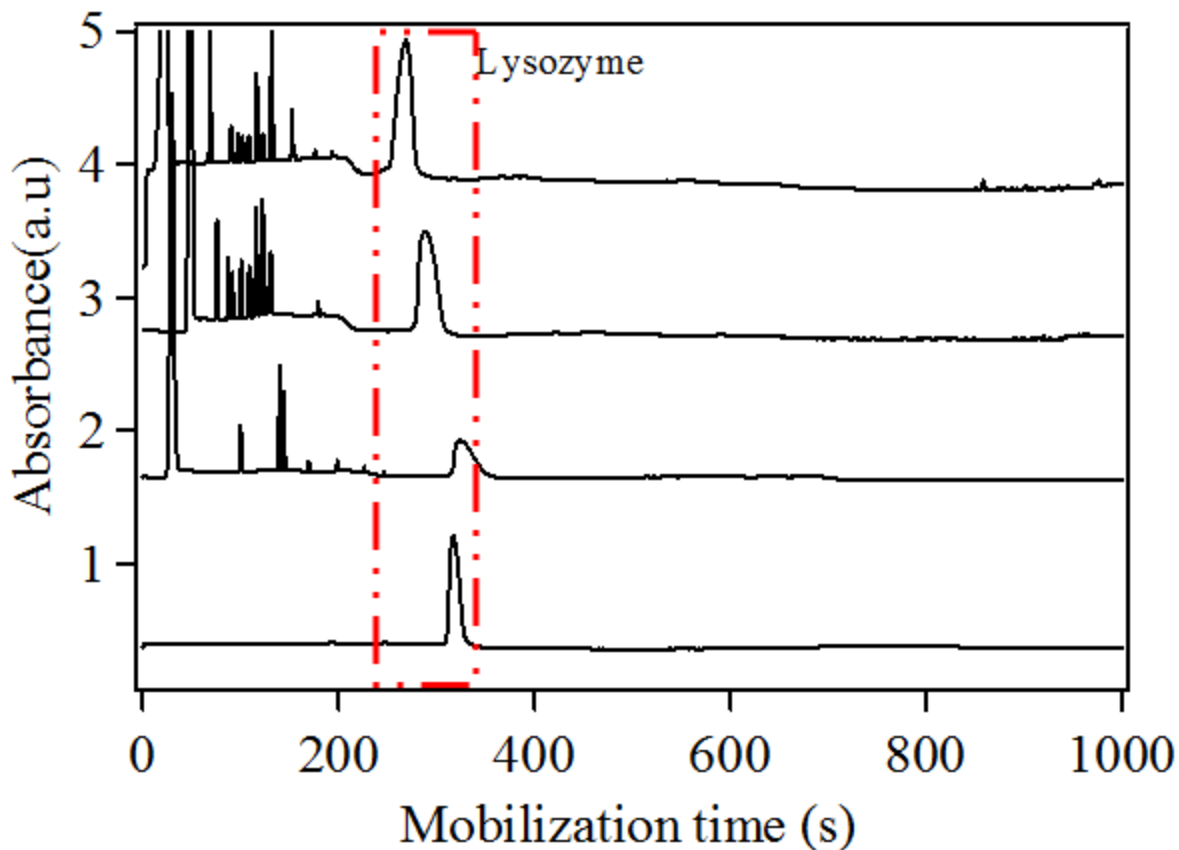
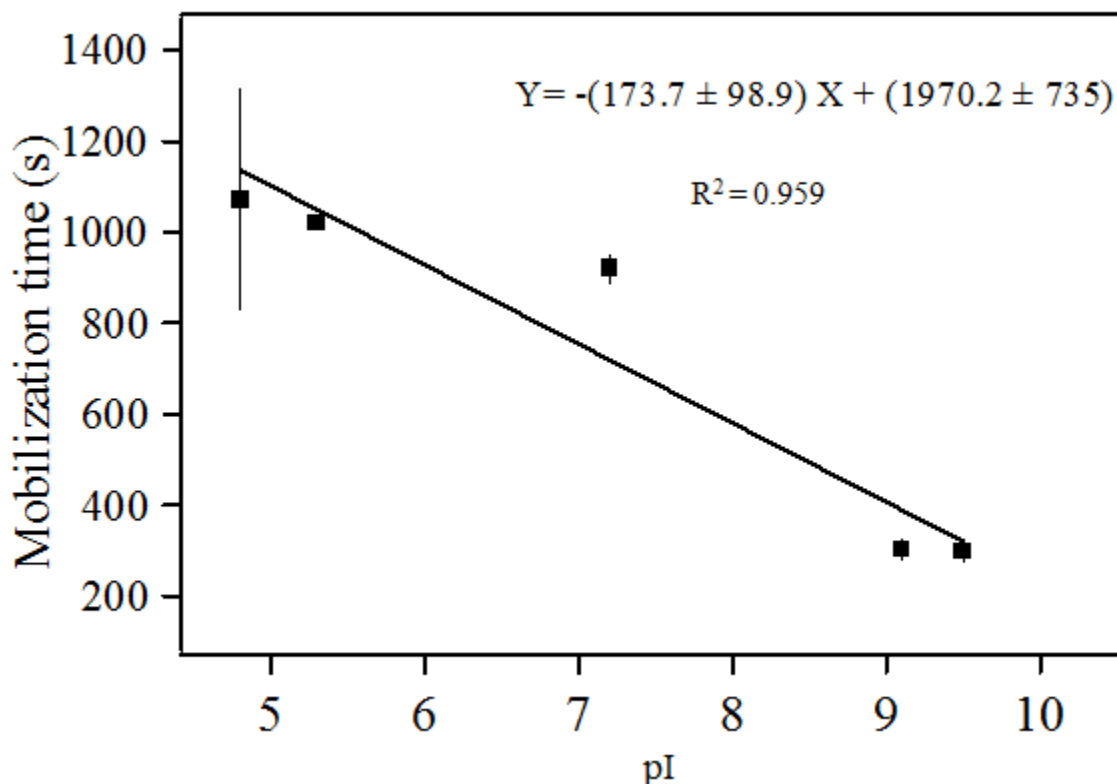


**Fig 3.4: Electropherogram of four consecutive runs of cIEF of Lysozyme in an EoTrol LN® coated capillary followed by anodic mobilization with neutral NaCl solution. Mobilization time of Lysozyme is  $299 \pm 22$  s with % RSD of 7.5.**

The plot of the pIs as a function of the mobilization times of the proteins is shown in Fig 3.5. The data were fit to a linear curve which produced a best fit line,  $Y = -173.5x + 1970.2$ . The correlation coefficient for the linear fit was 0.959. From the data observed, the bigger protein molecules seemed to have a higher tendency of being adsorbed on the surface; therefore BSA showed the highest standard deviation in mobilization times. In the literature, the same proteins from different animals or plants sources are reported to have different pI as provided in Table 3. From the data observed it can be said that the bigger protein molecule, the higher was the tendency of it being adsorbed on the surface; therefore BSA showed the highest standard deviation in mobilization times.

**Figure 3.5** Plot of mobilization time in observed experimentally against the reported pI values of standard proteins.



From the electropherograms obtained from the cIEF experiments with TR4 virus and T1 virus in Fig 3.6 and Fig 3.8, the mobilization times were  $798 (\pm 17)$  s and  $1450 (\pm 87)$  s respectively.

**Table 4: Calculation of pI of viruses based on their anodic mobilization times.**

virus	Capsid contents	mobilization time (s) (Y)	% RSD	Reported value pI(X)	Calcúlate (X= pI) Y= -173.4X+1970.4
TR4	RNA	$798 \pm 17$	2.2	$4.5 \pm 1.3$	$6.8 \pm 1.0$
T1	DNA	$1450 \pm 87$	4.4	$4.0 \pm 1.3$	$3.1 \pm 1.0$

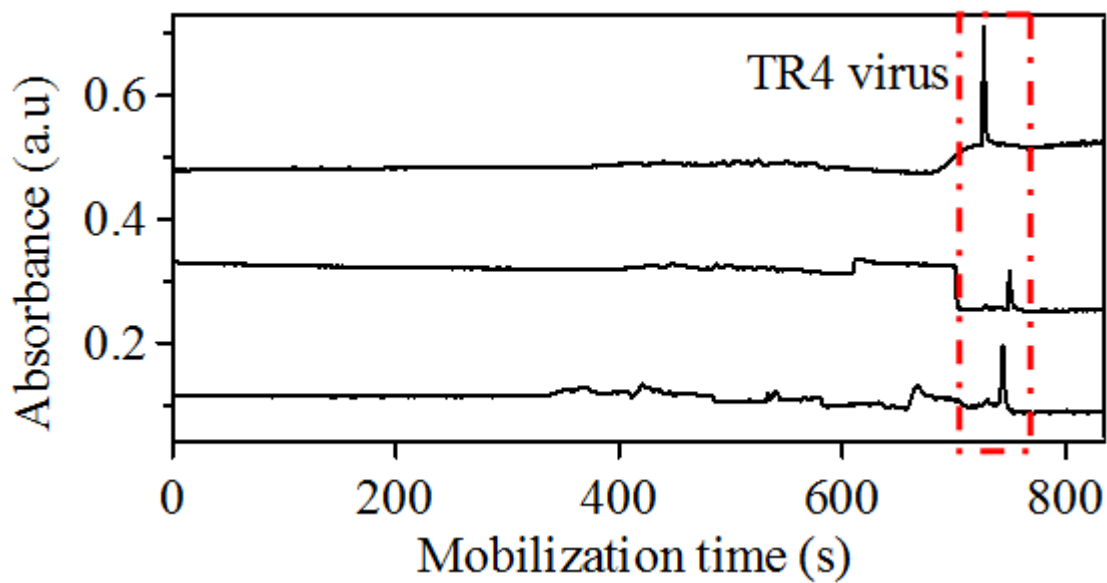


**Fig 3.6:** Electropherogram of three runs of TR4 virus detected by anodic mobilization after cIEF. Mobilization time is  $798 \pm 17$ s with 2.2% RSD.

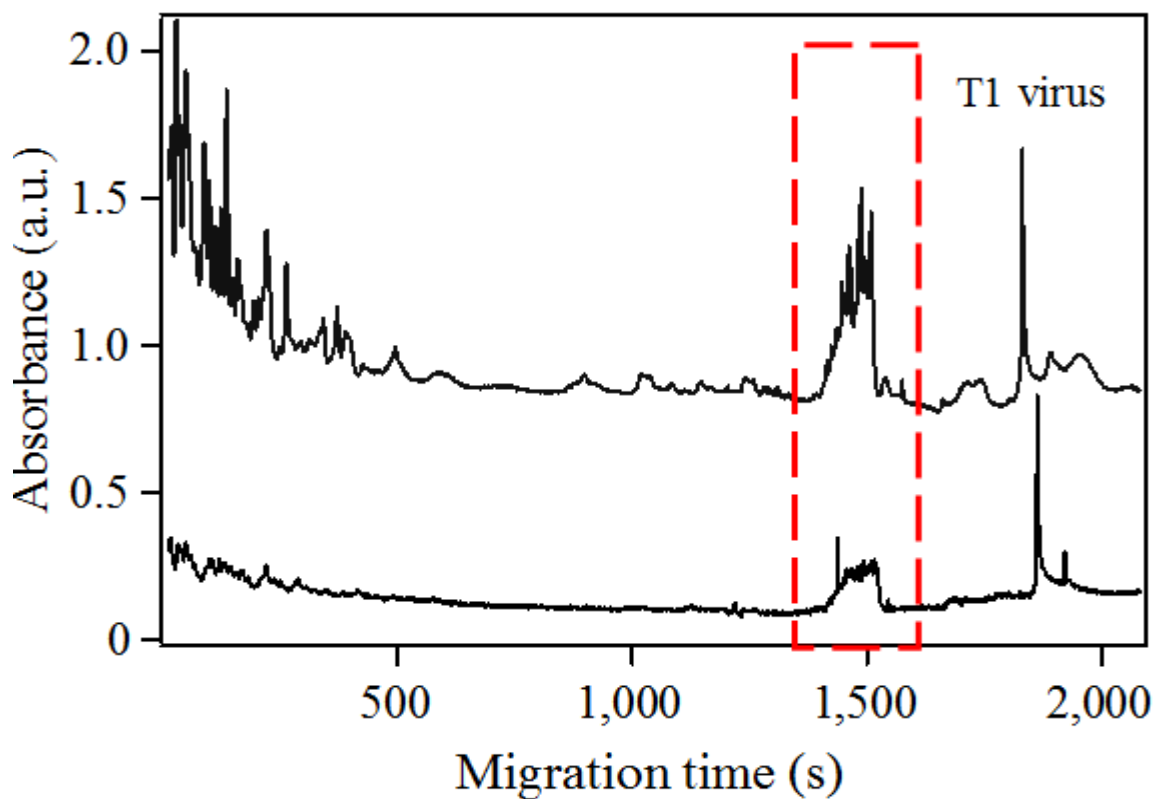


**Fig 3.7:** Electropherogram of T1 virus detected by anodic mobilization after cIEF. Migration times is  $1450 \pm 87$  s with 4.4 % RSD, a sharper peak at  $1850 \pm 20$  s.



The pI for TR4 virus,  $6.8 (\pm 1.0)$  pH units calculated from the equation of calibration curve based on the migration time. But in the electropherograms for the T1 viruses, two peaks were consistently observed; one at  $\sim 1450$  s and the other at  $\sim 1850$  s in all three consecutive runs. By increasing the detector sensitivity from 0.02 to 0.005, the broader peak S/N ratio didn't improve as shown in Fig 3.8. The two peaks in all electropherograms of T1 virus suggest that there are more than one analyte in the sample solution. The potential source of contamination in the sample might be the materials from the host bacteria that host the bacteriophage viruses in cell culture. This contamination either came from incomplete purification of virus sample or enough days were not provided for cell culture to form the significant amount of plaques (lyses of host bacteria with a lot of bacteriophage viruses) formation.<sup>82</sup> Just as an argument if the peak at  $\sim 1850$  s were considered, the pI it would correspond to 0.9 pH units which is much lower than the reported range of pI viruses from 1.5 to 9 pH units. While the peak at  $\sim 1450$  s corresponds to pI value of 3.0 which is reasonable close from the reported value of T1 virus. Since pI of viruses 0.9 is highly unlikely because pI values of different viruses measured by other methods have not been reported are within in the range of 3.5 to 8.5 pH units. In addition, pH range of ampholytes used in this experiment was between 3 to 10. Any peak which results pI value much lower than 3 or higher than from 10 must be from the contaminants. Hence, pI determination of T1 and TR4 viruses by above calculation must be very close to the true values,  $3.1 \pm 1.0$  and  $6.8 \pm 1.0$  pH units, although there is some degree of uncertainty exists due to experimental errors. However, the cIEF experiments with viruses need to be repeated before making final conclusions for detection and ascertainment of their pI values. Several papers have been published which report the successful detection of other viruses such as tobacco mosaic viruses<sup>83</sup> and influenza viruses<sup>84</sup> using cIEF method.

## Chapter 4 - Conclusions and future directions

Viral outbreaks causing hundreds of thousands of people to become sick have been a common occurrence.<sup>82</sup> A common method of detection and identification of viruses in various foods,<sup>85</sup> and infected people are the serology technique, cell culture, polymerized chain reaction (PCR) and electron microscopy. Serology involves detection of antibodies produced in the blood sample against the antigen. The PCR is a technique for isolating a DNA sequence by amplifying the selected DNA molecule from the mixture of other DNA molecules without purifying the mixture beforehand.<sup>86</sup> Amplification of target DNA requires several cycles of thermal treatment and synthesis reaction with tag polymerize with target nucleotide sequence. A complete cycle of this reaction requires at least a day. On the other hand, electron microscopy involves imaging of specimens to detect the presence of virus in the sample; the virus is identified based on its shape and size. Both methods, though widely used in clinical and research labs, require extensive sample preparation, long procedures, and expensive instruments. To meet the need for cheap and on-site detection technique of viruses and other pathogens, cIEF can be a viable option where various nano size pathogens can be detected and identified without exhaustive work for sample preparation and procedure.<sup>37</sup> From our preliminary work with cIEF, two bacteriophage viruses, T1 and TR4, have been detected and their pI has been determined as  $6.8 \pm 1.0$  and  $3.1 \pm 1.0$ . These values are within  $\pm 1.5$  of the range of reported pI values. The reported pI for different viruses differs by  $\pm 1.5$  depending upon the methods of detection and experimental conditions adopted. Developing an automated, efficient, portable, and disposable cIEF device to detect viruses on site is the major objective of this project. The main motivation of this project for future work is the detection of viruses and other pathogens on a poly (dimethylsiloxane) PDMS

chip by cIEF.<sup>87, 88</sup> Reasons behind choosing PDMS is that it is inexpensive, optically transparent, environmentally friendly and convenient for prototyping material. These PDMS devices also offer the capability of integrating multiple chemical processing steps along with the separations in a single device so that a complete chemical analysis can be performed on a chip. The advantages of such a strategy over conventional chemical analysis instrumentation include, 1) automation, 2) reduced consumption of reagents and analytes, 3) reduced waste generation, 4) high speed analysis with equivalent or increased performance, 5) operational simplicity and 6) compactness. Many different types of chemical manipulations and separations have been demonstrated on microfluidic devices which confirm these advantages, and several books and reviews have been written annually to report such progress.<sup>89</sup> Therefore, the future work of this project might involve a fabrication of quartz or PDMS or hybrid microchip for a rapid and inexpensive detection for wide range of infectious viruses, water and food borne pathogens by cIEF on channel of microchip.

## References

1. Han, C.; Yu, Z.; Feng, S.; Lv, D.; Yan, X.; Chen, G.; Li, X.; Ma, W.; Yan, Y. Applications of Capillary Electrophoresis for Rapidly Separating and Characterizing Water-soluble Proteins of Wheat Grains. *Cereal Research Communications* **2013**, *41*, 601-612.
2. Azadi, G.; Tripathi, A. Surfactant-induced electroosmotic flow in microfluidic capillaries. *Electrophoresis* **2012**, *33*, 2094-2101.
3. Chandler, J. M.; Trenary, H. R.; Walker, G. R.; Cooper, C. R. Capillary electrophoresis for protein profiling of the dimorphic, Pathogenic Fungus, *Penicillium marneffeii*. *Methods Mol. Biol.* **2013**, *984*, 275-84.
4. Kato, Masaru Toyo'oka, Toshimasa Gyoten, Yukari Sakai Kato, Kumiko Nakajima, Tohru Cationic starch derivatives as dynamic coating additives for analysis of amino acids and peptides using poly(methyl methacrylate) microfluidic devices. *Anal. Chem.* **2004**, *76*, 6792-6.
5. Anonymous <http://www.targetdiscovery.com/~tdidocs/EOTrolTechGuideRevC.pdf>.
6. Milanova, D.; Chambers, R.; Bahga, S.; Santiago, J. Electrophoretic mobility measurements of fluorescent dyes using on-chip capillary electrophoresis. *Electrophoresis* **2011**, *32*, 3286-3294.
7. Lagu, A. L. Applications of capillary electrophoresis in biotechnology. *Electrophoresis* **1999**, *20*, 3145-3155.
8. Paulson, J. R.; Higley, L. L. Acid-urea polyacrylamide slab gel electrophoresis of proteins: Preventing distortion of gel wells during preelectrophoresis. *Anal. Biochem.* **1999**, *268*, 157-159.
9. Matczuk, M.; Foteeva, L.; Jarosz, M.; Galanski, M.; Keppler, B.; Hirokawa, T.; Timerbaev, A. Can neutral analytes be concentrated by transient isotachopheresis in micellar electrokinetic chromatography and how much? *Journal of chromatography A* **2014**, *1345*, 212-218.
10. Jorgenson, J.; Lukacs, K. Capillary zone electrophoresis. *Science* **1983**, *222*, 266-272.
11. [www.wiki.com](http://www.wiki.com) .
12. Zhuravlev, L. T. The surface chemistry of amorphous silica. Zhuravlev model. *Colloids and surfaces.A, Physicochemical and engineering aspects* **2000**, *173*, 1-38.

13. Azam, M.; Darlington, A.; Gibbs Davis, J.; Azam, S. The influence of concentration on specific ion effects at the silica/water interface. *Journal of physics. Condensed matter* **2014**, *26*, 244107.
14. Grabbe, A.; Horn, R. Double-Layer and Hydration Forces Measured between Silica Sheets Subjected to Various Surface Treatments. *J. Colloid Interface Sci.* **1993**, *157*, 375-383.
15. Hiemstra, T. Variable Charge and Electrical Double Layer of Mineralâ“Water Interfaces: Silver Halides versus Metal (Hydr)Oxides. *Langmuir* **2012**, *28*, 15614-15623.
16. Hellqvist, A.; Hedeland, Y.; Pettersson, C. Evaluation of electroosmotic markers in aqueous and nonaqueous capillary electrophoresis. *Electrophoresis* **2013**, *34*, 3252-3259.
17. Mishchuk, N. A.; Gonzalez-Caballero, F. Nonstationary electroosmotic flow in open cylindrical capillaries. *Electrophoresis* **2006**, *27*, 650-660.
18. Lim, S.; Nan, H.; Lee, M.; Kang, S. Fast on-site diagnosis of influenza A virus by Palm PCR and portable capillary electrophoresis. *Journal of chromatography.B* **2014**, *963*, 134-139.
19. Dolnik, V.; Horvath, J.; Dolník, V. Polymer wall coatings for capillary electrophoresis. *Electrophoresis* **2001**, *22*, 644-655.
20. Horka, M.; Ruzicka, F.; Hola, V.; Kahle, V.; Moravcova, D.; Slais, K. Capillary Electromigration Separation of Proteins and Microorganisms Dynamically Modified by Chromophoric Nonionogenic Surfactant. *Anal. Chem.* **2009**, *81*, 6897-6904.
21. Harris, D. C. *Quantitative Chemical Analysis Sixth Edition W. H. Freeman and Co., New York; 2002.; .*
22. Hempel, G. Strategies to improve the sensitivity in capillary electrophoresis for the analysis of drugs in biological fluids. *Electrophoresis* **2000**, *21*, 691-698.
23. Steiner, F.; Scherer, B. Instrumentation for capillary electrochromatography. *Journal of chromatography A* **2000**, *887*, 55-83.
24. Harris, D., Ed.; In *Quantitative Chemical Analysis*; W.H. Freeman and Comapany: New York, 2007; .
25. Liu, Z.; Pawliszyn, J. Applications of capillary isoelectric focusing with liquid-core waveguide laser-induced fluorescence whole-column imaging detection. *Anal. Biochem.* **2005**, *336*, 94-101.

26. Ghanim, M.; Najimudin, N.; Ibrahim, K.; Abdullah, M. Low electric field DNA separation and in-channel amperometric detection by microchip capillary electrophoresis. *IET Nanobiotechnology* **2014**, *8*, 77-82.
27. Chandra, P.; Zaidi, S.; Noh, H.; Shim, Y. Separation and simultaneous detection of anticancer drugs in a microfluidic device with an amperometric biosensor. *Biosens. Bioelectron.* **2011**, *28*, 326-332.
28. Liu, Z.; Pawliszyn, J. Capillary isoelectric focusing with laser-induced fluorescence whole column imaging detection as a tool to monitor reactions of proteins. **2004**, *3*, 567-571.
29. Udseth, H. R.; Loo, J. A.; Smith, R. D. **1989**, *61*, 232.
30. Vesterberg, O.; Vesterberg, O.; Svensson, H.; Nevald, R.; Frank, V.; Brunvoll, J.; Bunnberg, E.; Djerassi, C.; Records, R. Isoelectric Fractionation, Analysis, and Characterization of Ampholytes in Natural pH Gradients. IV. Further Studies on the Resolving Power in Connection with Separation of Myoglobins. *Acta Chem. Scand.* **1966**, *20*, 820-834.
31. Hjerten, S.; Elenbring, K.; Kilar, F.; Liao, J. L.; Chen, A. J. C.; Siebert, C. J.; Zhu, M. D. Carrier-Free Zone Electrophoresis, Displacement Electrophoresis and Isoelectric-Focusing in a High-Performance Electrophoresis Apparatus. *J. Chromatogr.* **1987**, *403*, 47-61.
32. Pritchett, T. Capillary isoelectric focusing of proteins. *Electrophoresis* **1996**, *17*, 1195-1201.
33. Palm, A.; Zaragoza-Sundqvist, M.; Marko-Varga, G. Capillary isoelectric focusing of proteins utilizing poly(vinylpyrrolodone)- and plexigla-coated columns. **2004**, *27*, 124-128.
34. Slais, K.; Horka, M.; Karasek, P.; Planeta, J.; Roth, M. Isoelectric Focusing in Continuously Tapered Fused Silica Capillary Prepared by Etching with Supercritical Water. *Anal. Chem.* **2013**, *85*, 4296-4300.
35. Pager, C.; Vargova, A.; Takacsi-Nagy, A.; Doernyei, A.; Kilar, F. Effect of electrolyte pH on CIEF with narrow pH range ampholytes. *Electrophoresis* **2012**, *33*, 3269-3275.
36. Li, S.; Dong, J.; Guo, C.; Wu, Y.; Zhang, W.; Fan, L.; Cao, C.; Zhang, W. A stable and high-resolution isoelectric focusing capillary array device for micropreparative separation of proteins. *Talanta* **2013**, *116*, 259-265.
37. Horka, M.; Ruzicka, F.; Hola, V.; Slais, K. Capillary isoelectric focusing of microorganisms in the pH range 2-5 in a dynamically modified FS capillary with UV detection. *Analytical and Bioanalytical Chemistry* **2006**, *385*, 840-846.

38. Shiraishi, M.; Loutzenhiser, R.; Walsh, M. Analysis of myosin regulatory light chain phosphorylation by capillary isoelectric focusing with laser-induced fluorescence detection . **2004**, *86*, 390A-390A.
39. García-Campaña, A. M.; Gámiz-Gracia, L.; Baeyens, W. R. G.; Alés Barrero, F. Derivatization of biomolecules for chemiluminescent detection in capillary electrophoresis. *Journal of Chromatography B* **2003**, *793*, 49-74.
40. Haselberg, R.; de Jong, G. J.; Somsen, G. W. Capillary electrophoresis-mass spectrometry for the analysis of intact proteins. *Journal of Chromatography a* **2007**, *1159*, 81-109.
41. Khaledi, M. G. Capillary Isoelectric Focusing. **1998**, *49*, 223.
42. Wolken, G. G.; Kostal, V.; Arriaga, E. A. Capillary Isoelectric Focusing of Individual Mitochondria. *Anal. Chem.* **2011**, *83*, 612-618.
43. Jacobasch, H. J.; Kaden, H. Electrokinetic Phenomena - Fundamental Principles, Measuring Methods, Applications. *Zeitschrift Fur Chemie* **1983**, *23*, 81-91.
44. Huang, X. Y.; Ren, J. C. On-line chemiluminescence detection for isoelectric focusing of heme proteins on microchips. *Electrophoresis* **2005**, *26*, 3595-3601.
45. Huang, X.; Ren, J. On-line chemiluminescence detection for isoelectric focusing of heme proteins on microchips. *Electrophoresis* **2005**, *26*, 3595-3601.
46. Zhou, C. Characterization of human papillomavirus by capillary isoelectric focusing with whole-column imaging detection. *Electrophoresis* **2013**, *34*, 3046-3053.
47. Mao, Q.; Pawliszyn, J. Capillary isoelectric focusing with whole column imaging detection for analysis of proteins and peptides. *J. Biochem. Biophys. Methods* **1999**, *39*, 93-110.
48. Haselberg, R.; de Jong, G. J.; Somsen, G. W. Capillary electrophoresis-mass spectrometry for the analysis of intact proteins. *Journal of Chromatography a* **2007**, *1159*, 81-109.
49. Zhong, X.; Maxwell, E. J.; Ratnayake, C.; Mack, S.; Chen, D. D. Y. Flow-Through Microvial Facilitating Interface of Capillary Isoelectric Focusing and Electrospray Ionization Mass Spectrometry. *Anal. Chem.* **2011**, *83*, 8748-8755.
50. Hanrieder, J.; Zuberovic, A.; Bergquist, J. Surface modified capillary electrophoresis combined with in solution isoelectric focusing and MALDI-TOF/TOF MS: A gel-free multidimensional electrophoresis approach for proteomic profiling-Exemplified on human follicular fluid. *Journal of Chromatography a* **2009**, *1216*, 3621-3628.

51. Guillo, C.; Karlinsey, J. M.; Landers, J. P. On-chip pumping for pressure mobilization of the focused zones following microchip isoelectric focusing. *Lab on a Chip* **2007**, *7*, 112-118.
52. Taverna, M.; Chevalier, M.; Ferrier, D.; Tran, N. T. One-step capillary isoelectric focusing for the separation of the recombinant human immunodeficiency virus envelope glycoprotein glycoforms. *Journal of chromatography A* **2000**, *866*, 121-135.
53. Kleparnik, K.; Bocek, P. Electrophoresis today and tomorrow: helping biologists' dreams come true. *Bioessays* **2010**, *32*, 218-226.
54. Righetti, P. G.; Sebastiano, R.; Citterio, A. Capillary electrophoresis and isoelectric focusing in peptide and protein analysis. *Proteomics* **2013**, *13*, 325-340.
55. Manabe, T.; Miyamoto, H.; Iwasaki, A. Effects of catholytes on the mobilization of proteins after capillary isoelectric focusing. *Electrophoresis* **1997**, *18*, 92-97.
56. Dutta, D.; Ramsey, J. M. A microfluidic device for performing pressure-driven separations. *Lab on a Chip* **2011**, *11*, 3081-3088.
57. HASHIMOTO, M.; TSUKAGOSHI, K.; NAKAJIMA, R.; KONDO, K. Design of a Pressure-Mobilization System for Capillary Isoelectric Focusing-Chemiluminescence Detection. *Analytical Sciences* **1999**, *15*, 1281-1284.
58. Kang, J. Z.; Yan, J. L.; Liu, J. F.; Qiu, H. B.; Yin, X. B.; Yang, X. R.; Wang, E. K. Dynamic coating for resolving rhodamine B adsorption to poly (dimethylsiloxane)/glass hybrid chip with laser-induced fluorescence detection. *Talanta* **2005**, *66*, 1018-1024.
59. Cao, F.; Tan, L.; Xiang, L.; Liu, S.; Wang, Y. Application of the copolymers containing sulfobetaine methacrylate in protein separation by capillary electrophoresis. *Journal of Biomaterials Science-Polymer Edition* **2013**, *24*, 2058-2070.
60. Gassner, A.; Rudaz, S.; Schappler, J. Static coatings for the analysis of intact monoclonal antibody drugs by capillary zone electrophoresis. *Electrophoresis* **2013**, *34*, 2718-2724.
61. Dang, F. Q.; Kakehi, K.; Cheng, J. J.; Tabata, O.; Kurokawa, M.; Nakajima, K.; Ishikawa, M.; Baba, Y. Hybrid dynamic coating with n-dodecyl beta-D-maltoside and methyl cellulose for high-performance carbohydrate analysis on poly(methyl methacrylate) chips. *Anal. Chem.* **2006**, *78*, 1452-1458.
62. Garcia, C. D.; Dressen, B. M.; Henderson, A.; Henry, C. S. Comparison of surfactants for dynamic surface modification of poly(dimethylsiloxane) microchips. *Electrophoresis* **2005**, *26*, 703-709.



63. Bahnasy, M. F.; Lucy, C. A. A versatile semi-permanent sequential bilayer/diblock polymer coating for capillary isoelectric focusing. *Journal of Chromatography a* **2012**, *1267*, 89-95.
64. Righetti, P.; Gelfi, C.; Verzola, B.; Castelletti, L. The state of the art of dynamic coatings. *Electrophoresis* **2001**, *22*, 603-611.
65. Chang, W. W. P.; Bomberger, D. C.; Schneider, L. V. Improved CZE capabilities with new dynamic coatings. *Journal of capillary electrophoresis and microchip technology* **2005**, *9*, 53-6.
66. Hjertén, S.; Valtcheva, L.; Elenbring, K.; Liao, J. Fast, high-resolution (capillary) electrophoresis in buffers designed for high field strengths. *Electrophoresis* **1995**, *16*, 584-594.
67. KUCHAR, MCJ Liu, Peter Malik, Abdul Lee, Milton Polyacrylamide-modified polypropylene hollow fibers for capillary electrophoresis. *The journal of microcolumn separations* **1994**, *6*, 581-589.
68. Kaneta, T.; Ogura, T.; Yamato, S.; Imasaka, T. Band broadening of DNA fragments isolated by polyacrylamide gel electrophoresis in capillary electrophoresis. *Journal of Separation Science* **2012**, *35*, 431-435.
69. Krause, P. V., Kathleen Expert Knowledge in Intelligence Assessments: Bird Flu and Bioterrorism. *Int. Secur.* **2014**, *38*, 39-71.
70. Anonymous <http://www.microbiologybytes.com/introduction/structure.html>.
71. Anonymous <http://virology-online.com/viruses/Rhabdoviruses.htm>.
72. Proenca, M.; Proença, M.; Nunes, J. F. M.; de Matos, A. P. A. Texture Indicators for Segmentation of Polyomavirus Particles in Transmission Electron Microscopy Images. *Microscopy and microanalysis* **2013**, *19*, 1170-1182.
73. Anonymous [http://www.virology.net/big\\_virology/BVDNAmyo.html](http://www.virology.net/big_virology/BVDNAmyo.html).
74. Gamkrelidze, M.; D-àbrowska, K. T4 bacteriophage as a phage display platform. *Arch. Microbiol.* **2014**, *196*, 473-479.
75. Chong, Mun Chua, Anthony Jin Shun Tan, Terence Tze Tong Tan, Suat Ng, Mah Microscopy techniques in flavivirus research. *Micron* **2014**, *59*, 33-43.
76. Goodridge, L.; Goodridge, C.; Wu, J.; Griffiths, M.; Pawliszyn, J. Isoelectric Point Determination of Norovirus Virus-like Particles by Capillary Isoelectric Focusing with Whole Column Imaging Detection. *Anal. Chem.* **2004**, *76*, 48-52.

77. Kremser, L.; Blaas, D.; Kenndler, E. Capillary electrophoresis of biological particles: Viruses, bacteria, and eukaryotic cells. **2004**, *14*, 2282-2291.
78. Kremser, L. "Capillary Electrophoresis of Viruses, Subviral Particles and Virus Complexes". *Journal of Separation Science* **2007**, *30*, 1704.
79. Shen, Y.; Berger, S. J.; Smith, R. D. **2000**, *72*, 4607.
80. Nelson, R. E.; Lantz, A. W. Capillary isoelectric focusing of bacteria using cellulose coated capillaries. *Abstracts of Papers of the American Chemical Society* **2010**, 239.
81. Horka, M.; Kubicek, O.; Kubesova, A.; Rosenbergova, K.; Kubickova, Z.; Slais, K. Rapid separation and identification of the subtypes of swine and equine influenza A viruses by electromigration techniques with UV and fluorometric detection. *Analyst* **2011**, *136*, 3010-3015.
82. Dharmayanti, N. L. P. I.; Hartawan, R.; Wibawa, H.; Balish, A.; Donis, R.; Davis, C. T.; Samaan, G.; Pudjiatmoko; Hardiman Genetic Characterization of Clade 2.3.2.1 Avian Influenza A(H5N1) Viruses, Indonesia, 2012. *Emerging infectious diseases* **2014**, *20*, 677-80.
83. Kooyman, P.; Thompson, G. J. Characterization of Tobamoviruses Isolated from Tomatoes in South Africa. *Phytophylactica* **1990**, *22*, 265-268.
84. Horka, M.; Kubicek, O.; Kubesova, A.; Kubickova, Z.; Rosenbergova, K.; Slais, K. Testing of the influenza virus purification by CIEF. *Electrophoresis* **2010**, *31*, 331-338.
85. Davis, C.; Vally, H.; Bell, R.; Sheehan, F.; Beard, F. Viral gastrointestinal outbreaks in residential care facilities: an examination of the value of public health unit involvement. *Aust. N. Z. J. Public Health* **2014**, *38*, 177-83.
86. Yan, Y.; Wang, H.; Gao, L.; Ji, J.; Ge, Z.; Zhu, X.; He, P.; Chen, Z. A one-step multiplex real-time RT-PCR assay for rapid and simultaneous detection of human norovirus genogroup I, II and IV. *J. Virol. Methods* **2013**, *189*, 277-282.
87. Ou, J.; Ren, C. L. Microchip UV absorbance detection applied to isoelectric focusing of proteins. *Methods Mol. Biol.* **2013**, *949*, 507-21.
88. Shameli, S. M.; Elbuken, C.; Ou, J.; Ren, C. L.; Pawliszyn, J. Fully integrated PDMS/SU-8/quartz microfluidic chip with a novel macroporous poly dimethylsiloxane (PDMS) membrane for isoelectric focusing of proteins using whole-channel imaging detection. *Electrophoresis* **2011**, *32*, 333-339.

89. Salplachta, J.; Kubsova, A.; Horka, M. Latest improvements in CIEF: From proteins to microorganisms. *Proteomics* **2012**, *12*, 2927-2936.